

Normalized Wolfe-Powell-type local minimax method for finding multiple unstable solutions of nonlinear elliptic PDEs*

Wei Liu[†] Ziqing Xie[‡] Wenfan Yi[§]

Abstract

The local minimax method (LMM) proposed in [Y. Li and J. Zhou, SIAM J. Sci. Comput., 23(3), 840–865 (2001)] and [Y. Li and J. Zhou, SIAM J. Sci. Comput., 24(3), 865–885 (2002)] is an efficient method to solve nonlinear elliptic partial differential equations (PDEs) with certain variational structures for multiple solutions. The steepest descent direction and the Armijo-type step-size search rules are adopted in [Y. Li and J. Zhou, SIAM J. Sci. Comput., 24(3), 865–885 (2002)] and play a significant role in the performance and convergence analysis of traditional LMMs. In this paper, a new algorithm framework of the LMMs is established based on general descent directions and two normalized (strong) Wolfe-Powell-type step-size search rules. The corresponding algorithm framework named as the normalized Wolfe-Powell-type LMM (NWP-LMM) is introduced with its feasibility and global convergence rigorously justified for general descent directions. As a special case, the global convergence of the NWP-LMM algorithm combined with the preconditioned steepest descent (PSD) directions is also verified. Consequently, it extends the framework of traditional LMMs. In addition, conjugate gradient-type (CG-type) descent directions are utilized to speed up the NWP-LMM algorithm. Finally, extensive numerical results for several semilinear elliptic PDEs are reported to profile their multiple unstable solutions and compared for different algorithms in the LMM's family to indicate the effectiveness and robustness of our algorithms. In practice, the NWP-LMM combined with the CG-type direction indeed performs much better than its known LMM companions.

Key words. semilinear elliptic PDEs, multiple unstable solutions, local minimax method, normalized strong Wolfe-Powell-type search rule, conjugate gradient-type descent direction, general descent directions, global convergence

AMS subject classifications. 35J20, 35B38, 65N12, 65J15, 65Jxx

1 Introduction

Various nonlinear problems in physics, chemistry, biology and materials sciences can be reduced to consider multiple solutions of the Euler-Lagrange equation associated

*This work was supported by NSFC grants 12171148, 11771138 and the Construct Program of the Key Discipline in Hunan Province. Liu's work was also partially supported by the NSFC grants 12101252 and 11971007. Yi's work was also partially supported by the NSFC grant 11901185, National Key R&D Program of China (No. 2021YFA1001300) and the Fundamental Research Funds for the Central Universities 531118010207.

[†]Key Laboratory of Computing and Stochastic Mathematics (Ministry of Education), Hunan Normal University, Changsha, Hunan 410081, China. *Present address:* South China Research Center for Applied Mathematics and Interdisciplinary Studies, South China Normal University, Guangzhou 510631, China (Email: wliu@m.scnu.edu.cn).

[‡]Key Laboratory of Computing and Stochastic Mathematics (Ministry of Education), Hunan Normal University, Changsha, Hunan 410081, China (Email: ziqingxie@hnnu.edu.cn).

[§]Corresponding author. School of Mathematics, Hunan University, Changsha, Hunan 410082, China (Email: wfyi@hnu.edu.cn).

with a continuously Fréchet-differentiable nonlinear functional E defined on a real Hilbert space H , i.e.,

$$E'(u) = 0, \quad u \in H, \quad (1.1)$$

where E' is the Fréchet-derivative of E . Actually, solutions of the Euler-Lagrange equation (1.1) are called critical points of the functional E . The most well-known candidates for critical points are local extrema to which classical variational and optimization methods have contributed a lot.

Nowadays, with the development of new experimental techniques, it has been possible to observe local unstable equilibria or transient excited states in numerous physical/chemical/biological systems. Consequently, their theoretical and numerical studies have attracted increasing attentions [2, 5, 16, 25, 32, 38]. However, these local unstable equilibria or transient excited states are related to critical points that are not local extrema, and then called saddle points. Virtually, in terms of the instability analysis, for a critical point u_* with its second-order Fréchet-derivative $E''(u_*)$ existing, its instability can be depicted by its Morse index (MI) [2], which is defined as the maximal dimension of subspaces of H on which the linear operator $E''(u_*)$ is negative-definite. In fact, for a nondegenerate critical point u_* , i.e., $E''(u_*)$ is invertible, if its MI = 0, it is a strict local minimizer and then a stable critical point, while if its MI > 0, then it is an unstable critical point. Generally speaking, the higher MI means the more instability.

Owing to the instability and multiplicity of saddle points, the design and analysis of numerical methods for grasping saddle points in a stable way is much more challenging than that for stable critical points. In recent years, various numerical methods were developed to capture saddle points in a stable way, such as the (climbing) string method [10, 26], the gentlest ascent dynamics [11] and the (shrinking) dimer method [15, 37]. Nevertheless, the methods mentioned above mainly focus on finding saddle points with MI = 1.

In this paper, we are interested in stable and efficient numerical computations for multiple saddle points with high MIs. Existing methods in this area include the search extension method [3, 4] and its modified versions [21, 30], the augmented partial Newton method and its variants [19, 31], the high-index optimization-based shrinking dimer method [36] and its extension to non-gradient systems [35], etc.. Recently, some dynamical methods for finding constrained saddle points with high MIs were also developed [22, 34]. On the other hand, motivated by classical minimax theorems in the critical point theory (see, e.g., [25] and references therein) and numerical researches of Choi-McKenna [6], Ding-Costa-Chen [9] and Chen-Zhou-Ni [5], Li and Zhou proposed a local minimax method (LMM) for various high-MI saddle points based on a local minimax characterization of them [17]. Then in [32], Xie et al. modified the LMM with a significant relaxation on the domain of the *local peak selection*, which is a crucial notion for the LMM and will be illustrated in details later. According to [17, 32], the LMM grasps a saddle point with MI = n ($n \in \mathbb{N}^+$) by dealing with a two-level local minimax problem as

$$\min_{v \in S_H} \max_{w \in [L, v]} E(w), \quad (1.2)$$

where $S_H = \{v \in H : \|v\| = 1\}$ is the unit sphere with $\|\cdot\|$ the norm in H , $L \subset H$ is a given $(n-1)$ -dimensional closed subspace usually constructed based on some known or previously found critical points, and $[L, v] = \{tv + w_L : t \geq 0, w_L \in L\}$ denotes a closed half subspace. Actually, the inner local maximization is an optimization problem in the n -dimensional half subspace $[L, v]$, which can be solved efficiently by

standard optimization algorithms in Euclidean spaces. The outer constrained local minimization, which is generally infinite-dimensional and much more challenging in the numerical computation, is the major concern of the LMM. For the sake of handling this task, the LMM adopts a normalized iterative scheme (NIS) with the steepest descent direction $d_k^{SD} = -g_k$, i.e.,

$$v_{k+1} = v_k(\alpha_k) = \frac{v_k - \alpha_k g_k}{\|v_k - \alpha_k g_k\|}, \quad w_{k+1} = p(v_{k+1}), \quad k = 0, 1, 2, \dots, \quad (1.3)$$

where $\alpha_k > 0$ is a step-size and $g_k = \nabla E(w_k) \in H$ is the gradient of E at $w_k = p(v_k)$ with $p(v_k)$ representing a local maximizer of E on $[L, v_k]$, known as the so-called *local peak selection* of E w.r.t. L at v_k . Actually, the local peak selection $p(v_k)$ can be expressed as $p(v_k) = t_k v_k + w_k^L$ for some $t_k \geq 0$ and $w_k^L \in L$ [17].

One of fundamental problems for the NIS (1.3) is how to choose a suitable step-size α_k . In earliest implementations of the LMM, a normalized exact step-size search rule was employed and aimed to find the step-size $\alpha_k > 0$ such that the functional $E(p(v_k(\alpha)))$ attains its minimum [17], i.e.,

$$E(p(v_k(\alpha_k))) = \min_{\alpha > 0} E(p(v_k(\alpha))), \quad k = 0, 1, 2, \dots \quad (1.4)$$

Nevertheless, such a step-size search rule is very expensive in practical computations and it is even hard to establish the global convergence of the corresponding LMM algorithm. To compensate for this shortage, several normalized inexact step-size search rules with the advantages of low computational cost and easy implementation have been introduced in the literature to choose the step-size $\alpha_k > 0$ such that the decrease amount $E(p(v_k)) - E(p(v_k(\alpha_k))) > 0$ is acceptable.

Note that a widely applied normalized inexact step-size search rule in traditional LMMs is the normalized Armijo-type step-size search rule, which was first introduced in [18] and further simplified in [33] as the following form

$$E(p(v_k(\alpha_k))) \leq E(p(v_k)) - \frac{1}{4} \alpha_k t_k \|g_k\|^2, \quad k = 0, 1, 2, \dots \quad (1.5)$$

In fact, the factor $1/4$ can be replaced by any constant $\sigma \in (0, 1)$ [20]. Thanks to this step-size search rule, global convergence results for the normalized Armijo-type LMM (NA-LMM) algorithm were established in [18, 39]. However, the decrease condition (1.5) is satisfied for all sufficiently small step-sizes (see Fig. 1), hence some artificial safeguards are needed to prevent step-sizes from being too small and the algorithm from interminable backtracking [18, 39]. Actually, the backtracking strategy chooses the largest step-size in the sequence $\{\lambda \rho^m\}_{m \in \mathbb{N}}$ (for a given trial step-size $\lambda > 0$ and a backtracking factor $\rho \in (0, 1)$) that satisfies the normalized Armijo-type search rule. It plays an important role not only in the numerical implementation but also in the convergence analysis of the NA-LMM. Nevertheless, a choice of appropriate parameters λ and ρ is not known a priori. Recently, a normalized Goldstein-type step-size search rule was proposed in [20] to guarantee the sufficient decrease of the functional and prevent step-sizes from being too small simultaneously. The feasibility and global convergence analysis of the normalized Goldstein-type LMM (NG-LMM) were also provided in [20]. Actually, the normalized Goldstein-type step-size search rule in it makes progress with two inequalities, which can be formulated as

$$-\delta \alpha_k t_k \|g_k\|^2 \leq E(p(v_k(\alpha_k))) - E(p(v_k)) \leq -\sigma \alpha_k t_k \|g_k\|^2, \quad k = 0, 1, 2, \dots, \quad (1.6)$$

with constants σ and δ satisfying $0 < \sigma < \delta < 1$. Unfortunately, as shown in Fig. 1, the normalized Goldstein-type step-size search rule may exclude the minimizer α_*

of $E(p(v_k(\alpha)))$ outside the acceptable interval $[\bar{\alpha}_1, \bar{\alpha}_2]$. Thus, more effective and reasonable step-size search rules may devote to the LMM for credibly capturing saddle points of the functional E .

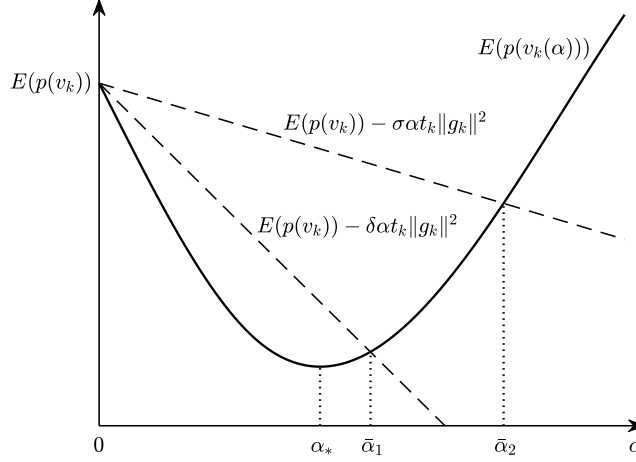


Figure 1: Illustration of normalized Armijo- and Goldstein-type step-size search rules in traditional LMMs: the acceptable interval of the Armijo-type step-size is $(0, \bar{\alpha}_2]$, while the acceptable interval of the Goldstein-type step-size is $[\bar{\alpha}_1, \bar{\alpha}_2]$.

Furthermore, the convergence rate is another fundamental problem of the NIS (1.3) for solving the outer minimization in the two-level local optimization problem (1.2). As shown in the NIS (1.3), the steepest descent direction $d_k^{SD} = -g_k = -\nabla E(p(v_k))$ was chosen as a descent direction in all existing LMM algorithms since 2001. As a result, they have certain limitations in terms of convergence rate. It is well known that, in line search algorithms for unconstrained optimizations in Euclidean spaces, there are many choices of descent directions that may have better performance than the steepest descent direction, such as the conjugate gradient (CG) direction and the quasi-Newton direction, which usually have rapid convergence rate. Therefore, in this paper we try to design some improved iterative schemes of the form as (1.3) by replacing the steepest descent direction $d_k^{SD} = -g_k$ by other more efficient descent directions $d_k \in H$ for the outer minimization process to improve the numerical performance and convergence rate of the LMMs' family. We note that the CG and quasi-Newton methods in optimization theory are often used in combination with some Wolfe-Powell line search strategy [24, 28, 29] that consists of the Armijo condition and a curvature condition. In fact, such a curvature condition on the step-size is particularly important for both algorithm implementation and convergence analysis of the CG and quasi-Newton methods.

Inspired by the discussions above, this paper is aimed to develop a new LMM framework based on general descent directions and the (strong) Wolfe-Powell-type step-size search rules, called a normalized Wolfe-Powell-type LMM (NWP-LMM), to capture multiple unstable solutions of the Euler-Lagrange equation (1.1) and provide the possibility to speed up the convergence. By employing some curvature properties, two types of normalized Wolfe-Powell-type step-size search rules will be introduced for the LMM with general descent directions. Their mathematical justifications and global convergence will be established rigorously for general descent directions by making full use of these curvature properties, which obviously distinguish from those of the NA-LMM [18, 32] and NG-LMM [20]. Finally, two types of descent directions, i.e., the preconditioned steepest descent (PSD) direction and the

CG-type descent direction, will be proposed and compared to be implemented in our NWP-LMM algorithm for computing multiple unstable solutions of several semilinear elliptic partial differential equations (PDEs), such as the nonlinear Schrödinger equation (NLSE), Hénon equation and Chandrasekhar equation. Indeed, it will be seen that the CG-type descent direction can greatly speed up our NWP-LMM algorithm. It is worthwhile to point out that the steepest descent direction can be replaced by a general descent direction in the devise of the traditional normalized Armijo-type and Goldstein-type LMM algorithms. Further, both the feasibility and global convergence of them can be verified in the line of our approach.

The rest of this paper is organized as follows. Firstly, some preliminaries for the LMM are provided in section 2. Then, in section 3, the NWP-LMM framework based on general descent directions and the normalized (strong) Wolfe-Powell-type step-size search rules is introduced. Its feasibility and some related properties are also discussed in this section. Global convergence of the NWP-LMM algorithm with general descent directions is verified rigorously in section 4. In addition, two different types of descent directions, i.e., the PSD and CG-type descent directions, are proposed and analyzed in section 5 to feasibly implement our NWP-LMM algorithms. Furthermore, section 6 reports the detailed numerical results in 2D including the numerical comparison of different LMM algorithms for above mentioned semilinear elliptic PDEs to illustrate the effectiveness and robustness of our approach. Finally, some conclusions are drawn in section 7.

2 Preliminaries

For the convenience of discussions later, we introduce some notations and basic lemmas for the LMM in this section.

Let (\cdot, \cdot) and $\|\cdot\|$ be respectively the inner product and norm in the Hilbert space H . Denote 2^H as the set of all subsets of the Hilbert space H , $S_H = \{v \in H : \|v\| = 1\}$ as the unit sphere in H and X^\perp as the orthogonal complement to a subspace $X \subset H$. Suppose that L , serving as a so-called support space later, is a given closed finite-dimensional subspace in H . Define the half subspace $[L, v] := \{tv + w^L : t \geq 0, w^L \in L\}$ for any $v \in S_H$. Throughout this paper, we assume that the functional E has a local minimizer at $0 \in H$ and focus on finding nontrivial saddle points of E . The *local peak selection*, a crucial notion, is defined as follows (cf. [17, 20, 32]).

Definition 2.1. *The peak mapping of E w.r.t. L is a set-valued mapping $P : S_H \rightarrow 2^H$ s.t., for any $v \in S_H$, $P(v)$ is the set of all local maximum points of E on $[L, v]$. A peak selection of E w.r.t. L is a single-valued mapping $p : S_H \rightarrow H$ s.t.*

$$p(v) \in P(v), \quad \forall v \in S_H.$$

For a given $v \in S_H$, we say that E has a local peak selection w.r.t. L at v if there is a neighborhood $\mathcal{N}(v)$ of v and a mapping $p : \mathcal{N}(v) \cap S_H \rightarrow H$ s.t.

$$p(u) \in P(u), \quad \forall u \in \mathcal{N}(v) \cap S_H.$$

Let $\langle \cdot, \cdot \rangle$ denote the duality pairing between H and its dual space H^* . By definition, each local peak selection $p(v)$, with $v \in S_H$, can be expressed as $p(v) = t_v v + w_v^L$ with $t_v \geq 0$ and $w_v^L \in L$. To avoid the degeneracy, we always assume that $t_v > 0$, i.e., $p(v) \notin L$, in the subsequent analysis. The above definition implies that $p(v)$ belongs to the well-known Nehari manifold $\mathcal{N}_E := \{u \in H \setminus \{0\} : \langle E'(u), u \rangle = 0\}$,

which contains all nontrivial critical points of the functional E . In fact, the following orthogonality holds obviously.

Lemma 2.2 ([20, 32]). *Assume that $E \in C^1(H, \mathbb{R})$ has a local peak selection p w.r.t. L at $v \in S_H$ satisfying $p(v) \notin L$. Then, $\langle E'(p(v)), w \rangle = 0$, $\forall w \in [L, v]$. In particular, $\langle E'(p(v)), p(v) \rangle = 0$.*

The following property follows from direct computation and is frequently utilized in the feasibility and convergence discussions for the LMM-type algorithms.

Lemma 2.3 ([20]). *Let $\bar{v} \in S_H \setminus L$. Suppose that the local peak selection p of E w.r.t. L is continuous at \bar{v} . Denote $p(v) = t_v v + w_v^L$ and $p(\bar{v}) = t_{\bar{v}} \bar{v} + w_{\bar{v}}^L$, where $t_v, t_{\bar{v}} \geq 0$ and $w_v^L, w_{\bar{v}}^L \in L$. If $v \rightarrow \bar{v}$, then $t_v \rightarrow t_{\bar{v}}$ and $w_v^L \rightarrow w_{\bar{v}}^L$.*

Imitating similar lines of the proof for Theorem 2.1 in [17], the following local minimax principle can be obtained and is referred to Theorem 4.1 in [20].

Theorem 2.4. *If $E \in C^1(H, \mathbb{R})$ has a local peak selection w.r.t. L at $\bar{v} \in S_H \setminus L$, denoted by $p(\bar{v}) = t_{\bar{v}} \bar{v} + w_{\bar{v}}^L$, satisfying (i) p is continuous at \bar{v} ; (ii) $t_{\bar{v}} > 0$; and (iii) \bar{v} is a local minimizer of $E(p(v))$ on S_H , then $p(\bar{v}) \notin L$ is a critical point of E .*

Since the local peak selection $p(\bar{v})$ is a local maximizer of E on the half subspace $[L, \bar{v}]$, Theorem 2.4 characterizes a saddle point of E as a solution to the local minimax problem (1.2), or equivalently, the local minimization problem of E on the solution submanifold

$$\mathcal{M} = \{p(v) : v \in S_H\}.$$

When a saddle point u^* of E (known as an unstable critical point in H) can be characterized as a local solution to the two-level optimization problem (1.2) of the form $u^* = p(v^*)$ with v^* minimizing $E(p(v))$ on S_H , it becomes stable on \mathcal{M} , i.e.,

$$E(u^*) = \min_{u \in \mathcal{M}} E(u). \quad (2.1)$$

We remark here that, under certain conditions, similar to Theorem 2.2 in [17] and Theorem 1.5 in [18], the existence of the local minimizer of $E(p(v))$ on a subspace of S_H can be verified by employing the Ekeland's variational principle. In addition, Theorem 2.4 also indicates an important feature of the LMM, which shows that it can stably find different saddle points and avoid computing those we have found. In fact, in order to obtain multiple saddle points, the LMM needs to repeatedly solve the local minimization problem (2.1) or the two-level local minimax problem (1.2) for different choices of L , which is usually spanned by some found critical points. Under assumptions of Theorem 2.4, a local minimizer of E on \mathcal{M} is a critical point different from those in L . As a result, Theorem 2.4 provides a mathematical justification that the LMM can find unstable saddle points of the functional E in a stable way.

Virtually, suitable descent algorithms can work for the minimization process in the optimization problem (1.2) or (2.1). As noted above, in traditional LMMs, the steepest descent direction serves as a search direction to numerically solve the local minimax problem (1.2). While, in this paper, the NWP-LMM will be constructed and analyzed for general descent directions.

3 Normalized Wolfe-Powell-type LMM

In this section, a NWP-LMM framework for general descent directions will be proposed to capture multiple saddle points of the functional E via solving the optimization problem (1.2). In order to hit this goal, two types of normalized Wolfe-Powell-type step-size search rules with general descent directions will be introduced and

where $\hat{t}_{v(\alpha)} = t_{v(\alpha)} / \sqrt{1 + \alpha^2 \|d\|^2}$.

Proof. The mean value theorem states that, when $s \in \mathbb{R}$ is close to zero,

$$\begin{aligned} E(p(v(\alpha + s))) - E(p(v(\alpha))) &= \langle E'(p(v(\alpha))), p(v(\alpha + s)) - p(v(\alpha)) \rangle \\ &= \langle E'(\xi) - E'(p(v(\alpha))), p(v(\alpha + s)) - p(v(\alpha)) \rangle \\ &\leq \|E'(\xi) - E'(p(v(\alpha)))\|_{H^*} \|p(v(\alpha + s)) - p(v(\alpha))\|, \end{aligned} \quad (3.4)$$

where $\xi = p(v(\alpha)) + \theta(p(v(\alpha + s)) - p(v(\alpha)))$ for some $\theta = \theta(\alpha) \in (0, 1)$. By the continuity of E' , p and $v(\alpha)$, we have

$$\|E'(\xi) - E'(p(v(\alpha)))\|_{H^*} \rightarrow 0 \quad \text{as } s \rightarrow 0.$$

The local Lipschitz continuity of p and Lemma 3.1 imply that the right-hand side of (3.4) is $o(\|p(v(\alpha + s)) - p(v(\alpha))\|) = o(\|v(\alpha + s) - v(\alpha)\|) = o(s\|d\|)$, and therefore, by Lemma 2.2,

$$\begin{aligned} E(p(v(\alpha + s))) - E(p(v(\alpha))) &= \langle E'(p(v(\alpha))), p(v(\alpha + s)) - p(v(\alpha)) \rangle + o(s\|d\|) \\ &= t_{v(\alpha+s)} \langle E'(p(v(\alpha))), v(\alpha + s) \rangle + o(s\|d\|) \\ &= \frac{t_{v(\alpha+s)} s}{\sqrt{1 + (\alpha + s)^2 \|d\|^2}} \langle E'(p(v(\alpha))), d \rangle + o(s\|d\|). \end{aligned}$$

From Lemma 2.3, we obtain $t_{v(\alpha+s)} \rightarrow t_{v(\alpha)}$ as $s \rightarrow 0$. It follows that

$$\lim_{s \rightarrow 0} \frac{E(p(v(\alpha + s))) - E(p(v(\alpha)))}{s} = \frac{t_{v(\alpha)}}{\sqrt{1 + \alpha^2 \|d\|^2}} \langle E'(p(v(\alpha))), d \rangle, \quad \alpha \in \mathbb{R}.$$

In other words, $E(p(v(\alpha)))$ is differentiable w.r.t. α and (3.3) holds. Finally, it is clear that the right-hand side of (3.3) is continuous w.r.t. α . The proof is completed. \square

Remark 3.3. If E possesses a higher regularity, say, $E \in C^1(H, \mathbb{R})$ and $E' : H \rightarrow H^*$ is locally γ_1 -Hölder continuous for some $\gamma_1 \in (0, 1]$, then the regularity assumption of p in Lemma 3.2 can be relaxed to that p is locally γ_2 -Hölder continuous around $v(\alpha)$ for some $\gamma_2 \in (1/(\gamma_1 + 1), 1]$. Actually, the key step in the proof is to justify that the right-hand side of (3.4) is $o(s\|d\|)$. The local Hölder continuity of E' and p implies that there exist two constants $C_1(\alpha), C_2(\alpha) > 0$ s.t., when $s \rightarrow 0$,

$$\begin{aligned} \|E'(\xi) - E'(p(v(\alpha)))\|_{H^*} \|p(v(\alpha + s)) - p(v(\alpha))\| &\leq C_1(\alpha) \|\xi - p(v(\alpha))\|^{\gamma_1} \|p(v(\alpha + s)) - p(v(\alpha))\| \\ &= C_1(\alpha) \theta^{\gamma_1} \|p(v(\alpha + s)) - p(v(\alpha))\|^{\gamma_1 + 1} \\ &\leq C_1(\alpha) C_2(\alpha) \|v(\alpha + s) - v(\alpha)\|^{\gamma_2(\gamma_1 + 1)}, \end{aligned}$$

where $\xi = p(v(\alpha)) + \theta(p(v(\alpha + s)) - p(v(\alpha)))$ and $\theta = \theta(\alpha) \in (0, 1)$ are the same as in (3.4). Consequently, the right-hand side of (3.4) is $o(s\|d\|)$.

3.1 Normalized Wolfe-Powell-type step-size search rules

Now, we are ready to propose normalized Wolfe-Powell-type step-size search rules for general descent directions by constructing curvature conditions to not only prevent step-sizes from being too small, but also avoid excluding the local minimizer of the function $E(p(v(\alpha)))$ w.r.t. α . In other words, the optimal step-size is always contained in the feasible step-size interval.

Definition 3.4 (Descent direction). *Let p be a local peak selection w.r.t. L at $v \in S_H \setminus L$. Assume that $E \in C^1(H, \mathbb{R})$ and $E'(p(v)) \neq 0$. A vector $d \in [L, v]^\perp$ is called a descent direction of E w.r.t. L at $p(v)$ if $\langle E'(p(v)), d \rangle < 0$.*

Remark 3.5. *It is noted that the above definition is slightly different from the usual definition of descent direction in optimization theory. In fact, the descent direction d in Definition 3.4 is not only required to decrease the functional E at $p(v)$ (i.e., $\langle E'(p(v)), d \rangle < 0$) but also to satisfy the orthogonality condition $d \perp [L, v]$. We make some comments on the reasons for introducing the latter condition as follows.*

- (i) *The descent direction d in Definition 3.4 is for the outer-level minimization and should be relatively independent of the inner-level maximization. Intuitively, an iteration along a descent direction in $[L, v]^\perp$, i.e., a descent direction with zero component in $[L, v]$, tends to enhance the stability of the algorithm.*
- (ii) *By Lemma 2.2, the condition $d \in [L, v]^\perp$ is automatically satisfied for the steepest descent direction $d^{SD} = -\nabla E(p(v))$ at $p(v)$, i.e., the Riesz representer of $-E'(p(v))$ determined by $(d^{SD}, \phi) = -\langle E'(p(v)), \phi \rangle$, $\forall \phi \in H$. Actually, this orthogonality plays a very important role in both algorithm implementation and theoretical analysis for the classical LMMs. Based on this observation, preserving this orthogonality to the general descent direction d for the outer-level minimization is a preferred choice.*

Definition 3.6 (Normalized Wolfe-Powell-type step-size search rules). *Suppose $E \in C^1(H, \mathbb{R})$ and let $v \in S_H \setminus L$, p be a peak selection of E w.r.t. L , and $d \in [L, v]^\perp$ be a descent direction of E w.r.t. L at $p(v)$. Denote $p(u) = t_u u + w_u^L$ ($u \in S_H$) with $t_u \geq 0$ and $w_u^L \in L$. For two given constants σ_1 and σ_2 with $0 < \sigma_1 < \sigma_2 < 1$, we say that the step-size $\alpha > 0$ satisfies*

- *the normalized Wolfe-Powell-type step-size search rule at v , if there hold*

$$E(p(v(\alpha))) \leq E(p(v)) + \sigma_1 \alpha t_v \langle E'(p(v)), d \rangle, \quad (3.5a)$$

$$\hat{t}_{v(\alpha)} \langle E'(p(v(\alpha))), d \rangle \geq \sigma_2 t_v \langle E'(p(v)), d \rangle, \quad (3.5b)$$

where $\hat{t}_{v(\alpha)} = t_{v(\alpha)} / \sqrt{1 + \alpha^2 \|d\|^2}$;

- *the normalized strong Wolfe-Powell-type step-size search rule at v , if there hold*

$$E(p(v(\alpha))) \leq E(p(v)) + \sigma_1 \alpha t_v \langle E'(p(v)), d \rangle, \quad (3.6a)$$

$$\hat{t}_{v(\alpha)} |\langle E'(p(v(\alpha))), d \rangle| \leq -\sigma_2 t_v \langle E'(p(v)), d \rangle. \quad (3.6b)$$

The condition (3.5a) or (3.6a) is referred to as the sufficient decrease condition, while conditions (3.5b) and (3.6b) are referred to as curvature conditions. It is pointed out that, if the steepest descent direction is employed, (3.5a) (or (3.6a)) is equivalent to the normalized Armijo-type condition used in traditional LMMs [18, 32, 33].

The feasibility of normalized (strong) Wolfe-Powell-type step-size search rules above is provided as follows.

Theorem 3.7. *Let $E \in C^1(H, \mathbb{R})$, $v \in S_H \setminus L$, $d \in [L, v]^\perp$ and p be a peak selection of E w.r.t. L . Denote $p(u) = t_u u + w_u^L$, $u \in S_H$, with $t_u \geq 0$ and $w_u^L \in L$. Assume that (i) p is locally Lipschitz continuous on the curve $\{v(\alpha) : \alpha \geq 0\}$; (ii) $t_v > 0$;*

(iii) d is a descent direction of E w.r.t. L at $p(v)$, i.e., $\langle E'(p(v)), d \rangle < 0$; and (iv) $\inf_{\alpha > 0} E(p(v(\alpha))) > -\infty$. Then, for given σ_1, σ_2 with $0 < \sigma_1 < \sigma_2 < 1$, there exist two positive constants $\bar{\alpha}_1, \bar{\alpha}_2$ with $\bar{\alpha}_1 < \bar{\alpha}_2$ s.t., for any $\alpha \in (\bar{\alpha}_1, \bar{\alpha}_2)$, it satisfies the normalized strong Wolfe-Powell-type step-size search rule (3.6) and therefore the normalized Wolfe-Powell-type step-size search rule (3.5).

Proof. Since (3.6) yields (3.5), we only need to verify that there exists an interval $(\bar{\alpha}_1, \bar{\alpha}_2)$ s.t. (3.6) holds for all $\alpha \in (\bar{\alpha}_1, \bar{\alpha}_2)$. Set $\varphi(\alpha) := E(p(v(\alpha)))$, $\alpha \geq 0$ and $\varphi(0) = E(p(v))$. In view of Lemma 2.3 and Lemma 3.2, we have $\varphi \in C^1([0, \infty), \mathbb{R})$ and $\varphi'(\alpha) = \hat{t}_{v(\alpha)} \langle E'(p(v(\alpha))), d \rangle$ with $\hat{t}_{v(\alpha)} = t_{v(\alpha)} / \sqrt{1 + \alpha^2 \|d\|^2}$. Note that conditions (ii) and (iii) imply $\varphi'(0) = t_v \langle E'(p(v)), d \rangle < 0$. Hence, (3.6) can be rewritten as

$$\varphi(\alpha) \leq \varphi(0) + \sigma_1 \alpha \varphi'(0), \quad |\varphi'(\alpha)| \leq -\sigma_2 \varphi'(0), \quad \alpha \geq 0, \quad (3.7)$$

and, for all $\alpha > 0$ small enough, $\varphi(\alpha) < \varphi(0) + \sigma_1 \alpha \varphi'(0)$ holds. In addition, since $\varphi(0) + \sigma_1 \alpha \varphi'(0) \rightarrow -\infty$ as $\alpha \rightarrow +\infty$ and the condition (iv) states that $\varphi(\alpha)$ is bounded from below for all $\alpha > 0$, apparently $\varphi(\alpha) > \varphi(0) + \sigma_1 \alpha \varphi'(0)$ holds for all $\alpha > 0$ large enough. Consequently, the equation

$$\varphi(\alpha) = \varphi(0) + \sigma_1 \alpha \varphi'(0), \alpha > 0, \quad (3.8)$$

admits at least one positive solution. Let $\bar{\alpha} > 0$ be the smallest positive solution to the equation (3.8). Then, it implies that

$$\varphi(\alpha) < \varphi(0) + \sigma_1 \alpha \varphi'(0), \quad \forall \alpha \in (0, \bar{\alpha}). \quad (3.9)$$

From the mean value theorem, there exists $\tilde{\alpha} \in (0, \bar{\alpha})$ s.t. $\varphi(\bar{\alpha}) - \varphi(0) = \varphi'(\tilde{\alpha})\bar{\alpha}$, which leads to $\varphi'(\tilde{\alpha}) = \sigma_1 \varphi'(0)$ by the definition of $\bar{\alpha}$. The facts that $0 < \sigma_1 < \sigma_2 < 1$ and $\varphi'(0) < 0$ imply that $\sigma_2 \varphi'(0) < \sigma_1 \varphi'(0) = \varphi'(\tilde{\alpha}) < 0$. Therefore, $|\varphi'(\tilde{\alpha})| < -\sigma_2 \varphi'(0)$. By the continuity of $\varphi'(\alpha)$, there exists $0 < \delta < \min\{\tilde{\alpha}, \bar{\alpha} - \tilde{\alpha}\}$ s.t.

$$|\varphi'(\alpha)| < -\sigma_2 \varphi'(0), \quad \forall \alpha \in (\tilde{\alpha} - \delta, \tilde{\alpha} + \delta) \subset (0, \bar{\alpha}). \quad (3.10)$$

Setting $\bar{\alpha}_1 = \tilde{\alpha} - \delta$ and $\bar{\alpha}_2 = \tilde{\alpha} + \delta$, the combination of (3.9)-(3.10) states that (3.7) holds for all $\alpha \in (\bar{\alpha}_1, \bar{\alpha}_2)$. \square

Remark 3.8. Fig. 3 provides a geometric interpretation of the feasibility of the normalized (strong) Wolfe-Powell-type step-size search rule.

3.2 Normalized Wolfe-Powell-type local minimax algorithm

Following the idea of traditional LMMs [17, 18, 32], the vital steps of the NWP-LMM algorithm are described in Algorithm 3.1.

Algorithm 3.1. Normalized Wolfe-Powell-type Local Minimax Algorithm.

Step 1. Take constants $\varepsilon > 0$, σ_1, σ_2 with $0 < \sigma_1 < \sigma_2 < 1$, and $n - 1$ previously found critical points u_1, u_2, \dots, u_{n-1} of E where u_{n-1} is the one with the highest critical value in $\{u_i\}$ ($1 \leq i \leq n-1$). Set $L = \text{span}\{u_1, u_2, \dots, u_{n-1}\}$, let $k := 0$, and choose an initial ascent direction $v_0 = v_0^L + v_0^\perp \in S_H$ at u_{n-1} with $v_0^L \in L$, $v_0^\perp \in L^\perp$ and $v_0^\perp \neq 0$. With an initial guess $w = v_0 + u_{n-1}$, solve for

$$w_0 = \arg \max_{w \in [L, v_0]} E(w),$$

and denote $w_0 = p(v_0) = t_0 v_0 + w_0^L$, where $t_0 \geq 0$ and $w_0^L \in L$.

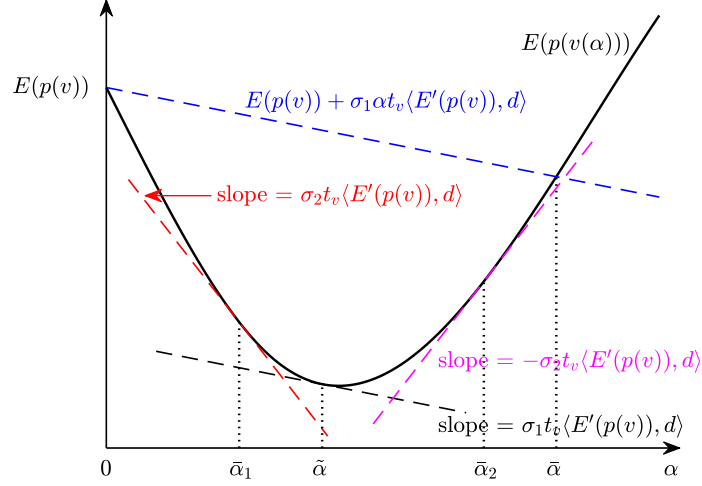


Figure 3: Illustration of the normalized (strong) Wolfe-Powell-type step-size search rule: the acceptable interval of the Wolfe-Powell-type step-size is $[\bar{\alpha}_1, \bar{\alpha}]$, while the acceptable interval of the strong Wolfe-Powell-type step-size is $[\bar{\alpha}_1, \bar{\alpha}_2]$. Here, only the case $\bar{\alpha}_2 \leq \bar{\alpha}$ is shown in the figure; for the case $\bar{\alpha}_2 > \bar{\alpha}$, we redefine $\bar{\alpha}_2 = \bar{\alpha}$.

Step 2. Compute a descent direction $d_k \in [L, v_k]^\perp$ of E w.r.t. L at $w_k = p(v_k)$ s.t. $\langle E'(w_k), d_k \rangle < 0$, which will be discussed in section 5.

Step 3. If the *stopping criterion* $\|E'(w_k)\|_{H^*} < \varepsilon$ is satisfied (or more criteria are satisfied if necessary), then output $u_n = w_k$ and stop; otherwise, go to **Step 4**.

Step 4. Set $v_k(\alpha) = \frac{v_k + \alpha d_k}{\|v_k + \alpha d_k\|}$ and find a step-size $\alpha_k > 0$ satisfying the normalized Wolfe-Powell-type step-size search rule, i.e.,

$$E(p(v_k(\alpha_k))) \leq E(w_k) + \sigma_1 \alpha_k t_k \langle E'(w_k), d_k \rangle, \quad (3.11a)$$

$$\hat{t}_k(\alpha_k) \langle E'(p(v_k(\alpha_k))), d_k \rangle \geq \sigma_2 t_k \langle E'(w_k), d_k \rangle, \quad (3.11b)$$

or the normalized strong Wolfe-Powell-type step-size search rule, i.e.,

$$E(p(v_k(\alpha_k))) \leq E(w_k) + \sigma_1 \alpha_k t_k \langle E'(w_k), d_k \rangle, \quad (3.12a)$$

$$\hat{t}_k(\alpha_k) |\langle E'(p(v_k(\alpha_k))), d_k \rangle| \leq -\sigma_2 t_k \langle E'(w_k), d_k \rangle, \quad (3.12b)$$

where $p(v_k(\alpha_k)) = t_k(\alpha_k) v_k(\alpha_k) + w_k^L(\alpha_k)$ with $t_k(\alpha_k) \geq 0$ and $w_k^L(\alpha_k) \in L$ is the local maximizer of E on $[L, v_k(\alpha_k)]$ computed by utilizing $w = t_k v_k(\alpha_k) + w_k^L$ as an initial guess and $\hat{t}_k(\alpha_k) = t_k(\alpha_k) / \sqrt{1 + \alpha_k^2 \|d_k\|^2}$.

Step 5. Set $v_{k+1} = v_k(\alpha_k)$, $t_{k+1} = t_k(\alpha_k)$, $w_{k+1}^L = w_k^L(\alpha_k)$ and $w_{k+1} = p(v_{k+1}) = t_{k+1} v_{k+1} + w_{k+1}^L$. Then, update $k := k + 1$ and go to **Step 2**.

We remark here that, similar to the classical (strong) Wolfe-Powell line search algorithm in optimization theory (see, e.g., [12, 23, 27]), one can employ an interpolation approach to efficiently find a step-size $\alpha_k > 0$ satisfying the normalized Wolfe-Powell-type step-size search rule (3.11) or the normalized strong Wolfe-Powell-type step-size search rule (3.12) in Step 4 of Algorithm 3.1. The implementation details are skipped here for brevity.

4 Global convergence

In this section, we establish the global convergence of Algorithm 3.1. In order to hit this goal, the following concept of compactness is needed. We simply utilize the same notations as those in Algorithm 3.1 throughout this section.

Definition 4.1 ([25]). *A functional $E \in C^1(H, \mathbb{R})$ is said to satisfy the Palais-Smale (PS) condition if every sequence $\{w_n\} \subset H$ s.t. $\{E(w_n)\}$ is bounded and $E'(w_n) \rightarrow 0$ in H^* has a convergent subsequence.*

It is pointed out that the following lemma gives a significant behavior of the sequence generated by Algorithm 3.1, which does not depend on the choice of descent directions and step-sizes in the algorithm. The proof is similar to that of Lemma 2.3 in [32] and omitted here for brevity.

Lemma 4.2. *Let $\{v_k\}$ be a sequence generated by Algorithm 3.1 with $v_0 \in S \setminus L$. Denote $v_k = v_k^\perp + v_k^L$ with $v_k^\perp \in L^\perp$ and $v_k^L \in L$, $k = 0, 1, \dots$, then there hold $\|v_0^\perp\| \leq \|v_k^\perp\| \leq 1$ and $v_k^L = \tau_k v_0^L$ with $0 < \tau_{k+1} \leq \tau_k \leq 1$ for $k = 0, 1, \dots$*

Lemma 4.2 states that once an initial ascent direction $v_0 = v_0^\perp + v_0^L \in S \setminus L$ is chosen in Algorithm 3.1, the closed subset

$$\mathcal{V}_0 := \{v = v^\perp + \tau v_0^L \in S_H : v^\perp \in L^\perp, 0 \leq \tau \leq 1\} \subset S_{[L^\perp, v_0^L]} \subset S_H \setminus L \quad (4.1)$$

contains all possible vectors v_k that Algorithm 3.1 may generate. Thus, the domain of a peak selection can be limited to be \mathcal{V}_0 instead of S_H .

We remark here that, in general, the local peak selection $p(v)$ defined on \mathcal{V}_0 is no longer a homeomorphism. The following weak version related to the homeomorphism property of the local peak selection $p(v)$ plays a significant role for establishing the global convergence. It can be verified by an analogous argument to that of Theorem 2.1 in [32] and only the continuity of the peak selection $p(v)$ on \mathcal{V}_0 is sufficient. Consequently, we skip the proof for simplicity.

Lemma 4.3. *Suppose $E \in C^1(H, \mathbb{R})$ and let p be a peak selection of E w.r.t. L satisfying (i) p is continuous on \mathcal{V}_0 and (ii) $t_k \geq \delta$ for some $\delta > 0$, $\forall k = 0, 1, \dots$. If the sequence $\{w_k\}$ generated by Algorithm 3.1 contains a subsequence $\{w_{k_i}\}$ converging to some $u_* \in H$, then the corresponding subsequence $\{v_{k_i}\}$ converges to some $v_* \in \mathcal{V}_0$ with $u_* = p(v_*)$.*

Before proving the global convergence of Algorithm 3.1, we give some assumptions on the general descent direction, which are quite reasonable and hold for many descent directions, especially for the steepest descent direction used in traditional LMMs.

$$(A1) \quad \langle E'(w_k), d_k \rangle \leq -c_1 \|E'(w_k)\|_{H^*}^2 \text{ for some } c_1 > 0, \forall k = 0, 1, \dots;$$

$$(A2) \quad \|d_k\| \leq c_2 \|E'(w_k)\|_{H^*} \text{ for some } c_2 > 0, \forall k = 0, 1, \dots;$$

$$(A3) \quad \text{if } \{v_k\} \text{ contains a subsequence } \{v_{k_i}\} \text{ converging to some } \bar{v} \text{ with } E'(p(\bar{v})) \neq 0, \\ \text{then the corresponding descent direction subsequence } \{d_{k_i}\} \text{ converges.}$$

Here, the assumption (A1) serves as a strong descent condition, and the assumption (A2) requires the length of the descent direction d_k to be controlled by that of the gradient. In addition, the assumption (A3) admits a certain weak version of the continuous dependency of the descent direction d_k on v_k .

The global convergence of Algorithm 3.1 is as follows.

Theorem 4.4. Suppose $E \in C^1(H, \mathbb{R})$ and let p be a peak selection of E w.r.t. L , $\{v_k\}$ and $\{w_k\}$ be sequences generated by Algorithm 3.1. If (i) p is locally Lipschitz continuous on \mathcal{V}_0 ; (ii) $t_k \geq \delta$ for some $\delta > 0$, $\forall k = 0, 1, \dots$; (iii) $\inf_{v \in \mathcal{V}_0} E(p(v)) > -\infty$ and assumptions (A1)-(A3) hold, then

- (a) $\sum_{k=0}^{\infty} \alpha_k \|E'(w_k)\|_{H^*}^2 < \infty$;
- (b) every accumulation point of $\{w_k\}$ is a critical point not belonging to L ;
- (c) $\liminf_{k \rightarrow \infty} \|E'(w_k)\|_{H^*} = 0$.

Further, if the functional E satisfies the (PS) condition, then

- (d) $\{w_k\}$ contains a subsequence converging to a critical point $u_* \notin L$. In addition, if u_* is isolated, then $w_k \rightarrow u_*$ as $k \rightarrow \infty$.

Proof. The decreasing condition (3.11a) (or (3.12a)), condition (ii) and assumption (A1) say that, for $k = 0, 1, \dots$,

$$E(w_{k+1}) - E(w_k) \leq \sigma_1 \alpha_k t_k \langle E'(w_k), d_k \rangle \leq -\sigma_1 \delta c_1 \alpha_k \|E'(w_k)\|_{H^*}^2. \quad (4.2)$$

Therefore, the sequence $\{E(w_k)\}$ is monotonically non-increasing. In addition, since the condition (iii) guarantees that $E(w_k)$ is bounded from below for all $k = 0, 1, \dots$, the sequence $\{E(w_k)\}$ converges to some $E_\infty := \inf_{k \geq 0} E(w_k)$.

Then, adding up (4.2), we can arrive at

$$\sum_{k=0}^{\infty} (E(w_{k+1}) - E(w_k)) \leq -\sigma_1 \delta c_1 \sum_{k=0}^{\infty} \alpha_k \|E'(w_k)\|_{H^*}^2. \quad (4.3)$$

Hence, the left-hand side of (4.3) converges to $E_\infty - E(w_0)$ which is finite. This immediately leads to the conclusion (a).

To prove the conclusion (b), let $\bar{u} \in H$ be an accumulation point of the sequence $\{w_k\}$. Then, there exists a subsequence $\{w_{k_i}\}$ converging to \bar{u} as $i \rightarrow \infty$. Recalling the weak version of the homeomorphism property in Lemma 4.3, it leads to that the corresponding subsequence $\{v_{k_i}\}$ converges to some $\bar{v} \in \mathcal{V}_0$ satisfying $\bar{u} = p(\bar{v}) = t_{\bar{v}} \bar{v} + w_{\bar{v}}^L$. Lemma 4.2 and the condition (ii) yield that, for some $\delta > 0$,

$$\text{dist}(\bar{u}, L) = \lim_{i \rightarrow \infty} \text{dist}(w_{k_i}, L) = \lim_{i \rightarrow \infty} t_{k_i} \|v_{k_i}^\perp\| \geq \delta \|v_0^\perp\| > 0,$$

and therefore $\bar{u} \notin L$.

The following is to verify that \bar{u} is a critical point by taking full advantages of the curvature condition (3.11b) (or (3.12b)), which states that

$$\frac{t_{k_i+1}}{\sqrt{1 + \alpha_{k_i}^2 \|d_{k_i}\|^2}} \langle E'(w_{k_i+1}), d_{k_i} \rangle \geq \sigma_2 t_{k_i} \langle E'(w_{k_i}), d_{k_i} \rangle, \quad i = 0, 1, \dots \quad (4.4)$$

By the contradiction argument, suppose that \bar{u} is not a critical point, i.e., $E'(\bar{u}) \neq 0$. Since the functional $E \in C^1(H, \mathbb{R})$, one can obtain

$$E'(w_{k_i}) \rightarrow E'(\bar{u}), \quad \text{as } i \rightarrow \infty. \quad (4.5)$$

As a result, for all i large enough, $\|E'(w_{k_i})\|_{H^*} > \|E'(\bar{u})\|_{H^*}/2 > 0$. In view of the conclusion (a), it leads to

$$\alpha_{k_i} \rightarrow 0, \quad \text{as } i \rightarrow \infty. \quad (4.6)$$

In addition, the assumption (A3) states that there exists $\bar{d} \in [L, \bar{v}]^\perp$ s.t.

$$d_{k_i} \rightarrow \bar{d}, \quad \text{as } i \rightarrow \infty. \quad (4.7)$$

Therefore, (4.6) and (4.7) immediately indicate that

$$v_{k_i+1} = \frac{v_{k_i} + \alpha_{k_i} d_{k_i}}{\sqrt{1 + \alpha_{k_i}^2 \|d_{k_i}\|^2}} \rightarrow \bar{v} \quad \text{in } H, \quad \text{as } i \rightarrow \infty,$$

and

$$E'(w_{k_i+1}) = E'(p(v_{k_i+1})) \rightarrow E'(p(\bar{v})) = E'(\bar{u}), \quad \text{as } i \rightarrow \infty, \quad (4.8)$$

holds by the continuity of E' and p . Moreover, reviewing Lemma 2.3 and the condition (ii), for some $\delta > 0$, we have

$$t_{k_i} \rightarrow t_{\bar{v}} \geq \delta > 0 \quad \text{and} \quad t_{k_i+1} \rightarrow t_{\bar{v}} \geq \delta > 0, \quad \text{as } i \rightarrow \infty. \quad (4.9)$$

Above all, combining (4.5)-(4.9) and taking $i \rightarrow \infty$ in (4.4) imply

$$t_{\bar{v}} \langle E'(\bar{u}), \bar{d} \rangle \geq \sigma_2 t_{\bar{v}} \langle E'(\bar{u}), \bar{d} \rangle. \quad (4.10)$$

Since $E'(\bar{u}) = E'(p(\bar{v})) \neq 0$, it follows from the assumption (A1), (4.5) and (4.7) that $\langle E'(\bar{u}), \bar{d} \rangle \leq -c_1 \|E'(\bar{u})\|_{H^*}^2 < 0$ for some $c_1 > 0$. Thus, we have $t_{\bar{v}} \langle E'(\bar{u}), \bar{d} \rangle < 0$ and (4.10) contradicts the fact $0 < \sigma_2 < 1$. Consequently, the accumulation point $\bar{u} = p(\bar{v})$ is a critical point. The conclusion (b) is obtained.

Next, we prove the conclusion (c) by the contradiction argument. Suppose that

$$\delta_1 := \liminf_{k \rightarrow \infty} \|E'(w_k)\|_{H^*} > 0.$$

Then, for k large enough, $\|E'(w_k)\|_{H^*} \geq \delta_1/2 > 0$. Thus, the conclusion (a) admits

$$\sum_{k=0}^{\infty} \alpha_k \|E'(w_k)\|_{H^*} < \infty. \quad (4.11)$$

In addition, Lemma 3.1 and the assumption (A2) yield that, for some $c_2 > 0$,

$$\|v_{k+1} - v_k\| = \|v_k(\alpha_k) - v_k\| \leq \alpha_k \|d_k\| \leq c_2 \alpha_k \|E'(w_k)\|_{H^*}, \quad k = 0, 1, \dots \quad (4.12)$$

Combining (4.11) and (4.12) results in $\sum_{k=0}^{\infty} \|v_{k+1} - v_k\| < \infty$. Therefore, $\{v_k\}$ is a Cauchy sequence in the closed subset \mathcal{V}_0 . Immediately, the completeness of the closed subset \mathcal{V}_0 implies that there exists $\bar{v} \in \mathcal{V}_0$ s.t. $v_k \rightarrow \bar{v}$ as $k \rightarrow \infty$. Further, by the continuity of p and E' , we have $w_k = p(v_k) \rightarrow p(\bar{v})$ with $p(\bar{v})$ the accumulation point, and $E'(w_k) \rightarrow E'(p(\bar{v}))$ as $k \rightarrow \infty$. Hence, there holds

$$\|E'(p(\bar{v}))\|_{H^*} = \lim_{k \rightarrow \infty} \|E'(w_k)\|_{H^*} = \delta_1 > 0.$$

This is a contradiction to the conclusion (b). Thus, the conclusion (c) is proved.

The rest is to prove the conclusion (d). Since $\{E(w_k)\}$ converges to E_∞ by the proof of the conclusion (a), according to the conclusion (c), there exists a subsequence $\{w_{k_i}\}$ s.t. $E(w_{k_i}) \rightarrow E_\infty$ and $E'(w_{k_i}) \rightarrow 0$ as $i \rightarrow \infty$. By the (PS) condition, $\{w_{k_i}\}$ possesses a subsequence, still denoted by $\{w_{k_i}\}$, that converges to a critical point $u_* \in H$. In addition, according to the conclusion (b), $u_* \notin L$ holds. Finally, under the assumption that u_* is isolated and following the analogous lines in the proof of Theorem 2.4 in [39] for the global convergence, the proof is completed. \square

5 Descent directions

In this section, we propose two specific types of descent directions for implementing Algorithm 3.1 in details. One is the PSD direction and the other is the CG-type descent direction. We use the same notations as those in Algorithm 3.1 for subsequent discussions in this section, unless specified.

5.1 Preconditioned steepest descent direction

The gradient of E at $w_k = p(v_k)$, denoted by $g_k = \nabla E(w_k)$, is defined by

$$(g_k, \phi) = \langle E'(p(v_k)), \phi \rangle, \quad \forall \phi \in H. \quad (5.1)$$

From the Riesz representation theorem, the gradient $g_k \in H$ exists uniquely and $\|g_k\| = \|E'(p(v_k))\|_{H^*}$. Consider the following PSD direction

$$d_k = -T_k g_k, \quad k = 0, 1, \dots, \quad (5.2)$$

where $T_k = T(v_k)$, called a preconditioner at v_k , is a positive-definite and self-adjoint bounded linear operator on H with an invariant subspace $[L, v_k]^\perp$. Assume that $T_k = T(v_k)$ satisfies

(T1) for some $c_3 > 0$, $\|T(v_k)u\| \leq c_3\|u\|$, $\forall u \in [L, v_k]^\perp$;

(T2) for some $c_4 > 0$, $(T(v_k)u, u) \geq c_4\|u\|^2$, $\forall u \in [L, v_k]^\perp$;

(T3) $T(v)$ is continuous at the accumulation point \bar{v} of $\{v_k\}$ s.t. $E'(p(\bar{v})) \neq 0$.

The following theorem provides the global convergence result of Algorithm 3.1 with d_k taken as the PSD direction (5.2).

Theorem 5.1. *Suppose $E \in C^1(H, \mathbb{R})$ and let p be a peak selection of E w.r.t. L , $\{v_k\}$ and $\{w_k\}$ be sequences generated by Algorithm 3.1 with $d_k = -T_k g_k$ the PSD direction defined in (5.2) and $T_k = T(v_k)$ satisfying assumptions (T1)-(T3). If (i) p is locally Lipschitz continuous on \mathcal{V}_0 ; (ii) $t_k \geq \delta$ for some $\delta > 0$, $\forall k = 0, 1, \dots$; and (iii) $\inf_{v \in \mathcal{V}_0} E(p(v)) > -\infty$, then those conclusions (a)-(d) in Theorem 4.4 hold.*

Proof. Since $g_k \in [L, v_k]^\perp$ from Lemma 2.2 and $[L, v_k]^\perp$ is an invariant subspace of $T_k = T(v_k)$, we have $d_k = -T_k g_k \in [L, v_k]^\perp$. In order to prove the conclusion, it suffices to verify assumptions (A1)-(A3) of Theorem 4.4. In fact, firstly, the assumption (T2) states that

$$\langle E'(w_k), d_k \rangle = -(g_k, T_k g_k) \leq -c_4 \|g_k\|^2 = -c_4 \|E'(w_k)\|_{H^*}^2, \quad k = 0, 1, \dots, \quad (5.3)$$

which is (A1) (with $c_4 = c_1$). Further, by the assumption (T1),

$$\|d_k\| = \|T_k g_k\| \leq c_3 \|g_k\| = c_3 \|E'(w_k)\|_{H^*}, \quad k = 0, 1, \dots \quad (5.4)$$

Thus, (A2) is verified by taking $c_3 = c_2$. Finally, (A3) directly follows from the assumption (T3) and the continuity of E' and p . \square

Taking T_k in Theorem 5.1 simply as the identity operator on H yields the following corollary, which draws the global convergence of Algorithm 3.1 with the standard steepest descent direction utilized at each iterative step.

Corollary 5.2. Suppose $E \in C^1(H, \mathbb{R})$ and let p be a peak selection of E w.r.t. L , $\{v_k\}$ and $\{w_k\}$ be sequences generated by Algorithm 3.1 with $d_k = -g_k$. If (i) p is locally Lipschitz continuous on \mathcal{V}_0 ; (ii) $t_k \geq \delta$ for some $\delta > 0$, $\forall k = 0, 1, \dots$; and (iii) $\inf_{v \in \mathcal{V}_0} E(p(v)) > -\infty$, then those conclusions (a)-(d) in Theorem 4.4 hold.

Remark 5.3. It is noted that Theorem 2.4 in [39], Theorem 5.1 in [20] and Corollary 5.2 provided respectively the global convergence of the NA-LMM, NG-LMM and NWP-LMM with the steepest descent direction. Consequently, mathematical justifications of LMMs combined with several typical inexact normalized step-size search rules for the steepest descent direction have been systematically established.

5.2 Conjugate gradient-type direction

For $k = 0, 1, \dots$, denote $v_k = v_k^L + v_k^\perp$ with $v_k^L \in L$ and $0 \neq v_k^\perp \in L^\perp$. Similar to the construction of the nonlinear CG method in the optimization theory (see, e.g., [7, 14]), we consider the following CG-type direction for Algorithm 3.1:

$$d_k = \begin{cases} -g_0, & k = 0, \\ -g_k + \beta_k \Pi_k d_{k-1}, & k \geq 1. \end{cases} \quad (5.5)$$

Here, $\beta_k \in \mathbb{R}$ is a parameter to be determined, $g_k = \nabla E(w_k)$ is the gradient of E at w_k defined in (5.1), and Π_k is the orthogonal projection from H onto $[L, v_k]^\perp$. Since $g_k \in [L, v_k]^\perp$ from Lemma 2.2, we have $d_k \in [L, v_k]^\perp$ for all $k \geq 0$. In addition, according to the definition of Π_k , it holds that $(g_k, \Pi_k d_{k-1}) = (g_k, d_{k-1})$, $k \geq 1$. Thus, the CG-type direction (5.5) satisfies

$$(g_k, d_k) = -\|g_k\|^2 + \beta_k (g_k, d_{k-1}), \quad k \geq 1. \quad (5.6)$$

Remark 5.4. We remark here that $\Pi_k d_{k-1}$ can be explicitly expressed as

$$\Pi_k d_{k-1} = d_{k-1} - \|v_k^\perp\|^{-2} (d_{k-1}, v_k^\perp) v_k^\perp, \quad k \geq 1. \quad (5.7)$$

Actually, by applying the facts that $d_{k-1} \in [L, v_{k-1}]^\perp \subset L^\perp$, $\Pi_k d_{k-1} \in [L, v_k]^\perp \subset L^\perp$, and $\text{Id} - \Pi_k$ is an orthogonal projection onto $([L, v_k]^\perp)^\perp = L \oplus [v_k^\perp]$, where Id is the identity operator on H and \oplus denotes the direct sum, we can conclude that

$$d_{k-1} - \Pi_k d_{k-1} \in ((L \oplus [v_k^\perp]) \cap L^\perp) = [v_k^\perp].$$

Thus, $d_{k-1} - \Pi_k d_{k-1} = c v_k^\perp$ for some $c \in \mathbb{R}$. Taking the inner product with v_k^\perp and noting that $(\Pi_k d_{k-1}, v_k^\perp) = (\Pi_k d_{k-1}, v_k - v_k^L) = 0$, we can obtain

$$(d_{k-1}, v_k^\perp) = (d_{k-1} - \Pi_k d_{k-1}, v_k^\perp) = c \|v_k^\perp\|^2,$$

yielding $c = \|v_k^\perp\|^{-2} (d_{k-1}, v_k^\perp)$. Consequently, the expression (5.7) is true.

The following lemma shows that, if the exact step-size search rule is applied in the previous iteration, the CG-type direction (5.5) with an arbitrary parameter β_k is a descent direction.

Lemma 5.5. For $k \geq 1$, let $v_k = v_{k-1}(\alpha_{k-1})$ with d_k defined in (5.5) and $\alpha_{k-1} > 0$ a local minimizer of $E(p(v_{k-1}(\alpha)))$ along $\{\alpha : \alpha > 0\}$. If $E \in C^1(H, \mathbb{R})$, p is locally Lipschitz continuous around v_k , and $t_k > 0$, then $(g_k, d_k) = -\|g_k\|^2$.

Proof. From Lemma 3.2, $E(p(v_{k-1}(\alpha)))$ is continuously differentiable at $\alpha = \alpha_{k-1}$ and

$$\left. \frac{d}{d\alpha} E(p(v_{k-1}(\alpha))) \right|_{\alpha=\alpha_{k-1}} = \frac{t_k}{\sqrt{1 + \alpha_{k-1}^2 \|d_{k-1}\|^2}} \langle E'(p(v_k)), d_{k-1} \rangle.$$

By applying the facts that $t_k > 0$ and $E(p(v_{k-1}(\alpha)))$ attains its local minimum at α_{k-1} , we have $\langle E'(p(v_k)), d_{k-1} \rangle = (g_k, d_{k-1}) = 0$. Thus, the conclusion follows from (5.6) immediately. \square

Due to the fact that the exact step-size search rule is quite expensive in practical computations, we focus on how to ensure that the CG-type direction d_k defined in (5.5) is a descent direction when a suitable inexact step-size search rule is used.

Inspired by the well-known Fletcher-Reeves CG method [13] in the optimization theory, we set

$$\beta_k^{\text{FR-like}} = \frac{\gamma_k \|g_k\|^2}{\|g_{k-1}\|^2}, \quad k \geq 1, \quad (5.8)$$

where $\gamma_k = \hat{t}_k/t_{k-1}$ with $\hat{t}_k = t_k/\sqrt{1 + \alpha_{k-1}^2 \|d_{k-1}\|^2}$. It can be verified that the CG-type direction (5.5) with $\beta_k = \beta_k^{\text{FR-like}}$ is a descent direction if the step-size α_k in each iteration satisfies the normalized strong Wolfe-Powell-type step-size search rule (3.12) with $\sigma_2 \in (0, 1/2)$, as stated in the following lemma. The proof follows the lines of the proof for Theorem 1 in [1].

Lemma 5.6. *For $k = 0, 1, \dots$, if $g_k \neq 0$, d_k in Algorithm 3.1 is defined in (5.5) with $\beta_k = \beta_k^{\text{FR-like}}$, and α_k is determined by the normalized strong Wolfe-Powell-type step-size search rule (3.12) with $\sigma_2 \in (0, 1/2)$, then*

$$-\frac{1 - \sigma_2^{k+1}}{1 - \sigma_2} \leq \frac{(g_k, d_k)}{\|g_k\|^2} \leq -\frac{1 - 2\sigma_2 + \sigma_2^{k+1}}{1 - \sigma_2}, \quad k = 0, 1, \dots \quad (5.9)$$

Consequently,

$$(g_k, d_k) < 0, \quad k = 0, 1, \dots \quad (5.10)$$

Proof. For $k = 0$, $d_0 = -g_0$, conclusions (5.9) and (5.10) are obvious. According to the inductive argument, suppose that conclusions (5.9) and (5.10) hold for $k - 1$ ($k \geq 1$). In view of the definition of $\beta_k^{\text{FR-like}}$ in (5.8), the fact (5.6) yields

$$\frac{(g_k, d_k)}{\|g_k\|^2} = -1 + \gamma_k \frac{(g_k, d_{k-1})}{\|g_{k-1}\|^2}, \quad k \geq 1.$$

Using the inductive assumption (5.10) for $k - 1$ ($k \geq 1$), the normalized strong Wolfe-Powell-type step-size search rule (3.12) states that

$$\gamma_k |(g_k, d_{k-1})| \leq -\sigma_2 (g_{k-1}, d_{k-1}),$$

and therefore,

$$-1 + \sigma_2 \frac{(g_{k-1}, d_{k-1})}{\|g_{k-1}\|^2} \leq \frac{(g_k, d_k)}{\|g_k\|^2} \leq -1 - \sigma_2 \frac{(g_{k-1}, d_{k-1})}{\|g_{k-1}\|^2}.$$

Further, by the inductive assumption (5.9) for $k - 1$ ($k \geq 1$), we can arrive at

$$-\frac{1 - \sigma_2^{k+1}}{1 - \sigma_2} = -1 - \sigma_2 \frac{1 - \sigma_2^k}{1 - \sigma_2} \leq \frac{(g_k, d_k)}{\|g_k\|^2} \leq -1 + \sigma_2 \frac{1 - \sigma_2^k}{1 - \sigma_2} = -\frac{1 - 2\sigma_2 + \sigma_2^{k+1}}{1 - \sigma_2},$$

which leads to the conclusion (5.9) for $k \geq 1$. Since $\sigma_2 \in (0, 1/2)$, it immediately follows that $(g_k, d_k) < 0$, $k \geq 1$. The proof is finished by the inductive argument. \square

Remark 5.7. Under assumptions in Lemma 5.6, we have from (5.9) that $(g_k, d_k) \leq -c_1 \|g_k\|^2$ with $c_1 = (1 - 2\sigma_2)/(1 - \sigma_2) > 0$, i.e., the CG-type direction (5.5) with $\beta_k = \beta_k^{\text{FR-like}}$ satisfies the assumption (A1) in Theorem 4.4. Moreover, under the same assumptions, these conclusions in Lemma 5.6 can be extended directly to any choice of β_k satisfying $|\beta_k| \leq \beta_k^{\text{FR-like}}$.

Remark 5.8. It is currently unclear whether assumptions (A2) and (A3) in Theorem 4.4 hold for the NWP-LMM with the CG-type descent direction (5.5). Thus, the global convergence of it has not been verified yet and will be our future work. Indeed, the NWP-LMM with the CG-type descent direction (5.5) is very efficient for finding multiple solutions of semilinear elliptic PDEs, compared to traditional LMMs and the NWP-LMM with the steepest descent direction, which will be shown in the section 6. Actually, several different constructions of CG-type descent directions can also be designed based on similar ideas of various CG methods in the optimization theory, which can be found, e.g., in [7, 14].

6 Numerical examples

In this section, we apply our NWP-LMM to find multiple unstable solutions of the semilinear elliptic boundary value problem (BVP)

$$\begin{cases} -\Delta u(\mathbf{x}) + a(\mathbf{x})u(\mathbf{x}) = f(\mathbf{x}, u(\mathbf{x})), & \mathbf{x} \in \Omega, \\ u(\mathbf{x}) = 0, & \mathbf{x} \in \partial\Omega, \end{cases} \quad (6.1)$$

where Ω is a bounded domain in \mathbb{R}^N with a Lipschitz boundary $\partial\Omega$, $a \in L^\infty(\Omega)$ and $a(\mathbf{x}) \geq 0$ ($\mathbf{x} \in \Omega$), and $f : \bar{\Omega} \times \mathbb{R} \rightarrow \mathbb{R}$ satisfies the following standard hypotheses [25]:

- (f1) $f(\mathbf{x}, \xi)$ is locally Lipschitz on $\bar{\Omega} \times \mathbb{R}$;
- (f2) there is a constant $c > 0$ s.t. $|f(\mathbf{x}, \xi)| \leq c(1 + |\xi|^{s-1})$ for some $s \in (2, 2^*)$, where $2^* := 2N/(N - 2)$, if $N \geq 3$; and $2^* := \infty$, if $N = 1, 2$;
- (f3) there are constants $\mu > 2$ and $R > 0$ s.t., for $|\xi| \geq R$, $0 < \mu F(\mathbf{x}, \xi) \leq f(\mathbf{x}, \xi)\xi$, where $F(\mathbf{x}, \xi) = \int_0^\xi f(\mathbf{x}, t)dt$;
- (f4) $f(\mathbf{x}, \xi) = o(\xi)$ as $\xi \rightarrow 0$.

Define $H = H_0^1(\Omega)$ with the a -dependent inner product and norm as

$$(u, v)_a = \int_{\Omega} \left(\nabla u(\mathbf{x}) \cdot \nabla v(\mathbf{x}) + a(\mathbf{x})u(\mathbf{x})v(\mathbf{x}) \right) d\mathbf{x}, \quad \|u\|_a = \sqrt{(u, u)_a}. \quad (6.2)$$

Since $a(\mathbf{x})$ is nonnegative and uniformly bounded, the norm $\|\cdot\|_a$ is equivalent to the usual norm in $H_0^1(\Omega)$, i.e., $\|u\| = \left(\int_{\Omega} |\nabla u(\mathbf{x})|^2 d\mathbf{x} \right)^{1/2}$. The variational energy functional associated to the BVP (6.1) is given as

$$E(u) = \int_{\Omega} \left(\frac{1}{2} (|\nabla u(\mathbf{x})|^2 + a(\mathbf{x})|u(\mathbf{x})|^2) - F(\mathbf{x}, u(\mathbf{x})) \right) d\mathbf{x} = \frac{1}{2} \|u\|_a^2 - \int_{\Omega} F(\mathbf{x}, u(\mathbf{x})) d\mathbf{x}.$$

It is well known that, under hypotheses (f1)-(f4), $E \in C^1(H, \mathbb{R})$ and satisfies the (PS) condition. Each critical point of E is a weak solution and also a classical solution to the BVP (6.1) [25]. In addition, $u \equiv 0$ is a local minimizer of E . Moreover, in any finite-dimensional subspace of H , $E(u) \rightarrow -\infty$ uniformly as $\|u\|_a \rightarrow \infty$. Hence, for any finite-dimensional closed subspace L , the peak mapping P of E w.r.t. L is nonempty. According to [17], we assume, in addition to hypotheses (f1)-(f4), that

(f5) $f(x, \xi)/|\xi|$ is increasing w.r.t. ξ on $\mathbb{R} \setminus \{0\}$.

For $L = \{0\}$, as shown in [17], under hypotheses (f1)-(f5), E has only one local maximizer in any direction, i.e., E has a unique peak selection $p(v) = t_v v$ ($\forall v \in S_H$) w.r.t. $L = \{0\}$. Moreover, there exists $\delta > 0$ s.t. $t_v = \|p(v)\| \geq \delta$ for any $v \in S_H$, that is exactly the separation condition in Theorem 4.4 when $L = \{0\}$. For any finite-dimensional closed subspace L , the uniqueness of the peak selection of E w.r.t. L implies its continuity. As a result, the unique peak selection p w.r.t. $L = \{0\}$ is continuous on S_H . Moreover, if conditions (f1)-(f5) hold and

(f6) $f(x, \xi)$ is C^1 and there exists a constant $\tilde{c} > 0$ s.t. $|f_\xi(x, \xi)| \leq \tilde{c}(1 + |\xi|^{s-2})$, for s as specified in (f2),

then the unique peak selection p w.r.t. $L = \{0\}$ is C^1 [17].

Due to the limit of the length of the paper, numerical experiments mainly focus on the following three cases of the BVP (6.1) on a 2D domain (a square or dumbbell-shaped domain).

Case 1. (*NLSE in the focusing regime* [8]) $f(\mathbf{x}, u) = u^3$, $a(\mathbf{x}) = \omega|\mathbf{x}|^2$ with $\omega > 0$ and $|\mathbf{x}| := \sqrt{x_1^2 + x_2^2}$ for all $\mathbf{x} = (x_1, x_2) \in \Omega = (-1, 1)^2 \subset \mathbb{R}^2$.

Case 2. (*Hénon equation* [5, 18]) $a(\mathbf{x}) = 0$, $f(\mathbf{x}, u) = |\mathbf{x}|^\ell u^3$ ($\ell \geq 0$) and $\Omega = (-1, 1)^2$.

Case 3. (*Chandrasekhar equation* [5]) $a(\mathbf{x}) = 0$, $f(\mathbf{x}, u) = (u^2 + 2u)^{3/2}$, $u \geq 0$ and Ω is a 2D dumbbell-shaped domain as described later.

It is clear that hypotheses (f1)-(f6) hold for all functions f in Cases 1-3. In addition, our approach is efficient for different domains such as a L-shaped domain, a ball or other complex domains in high dimensions.

In our numerical experiments, the initial ascent direction v_0 is taken as $v_0 = \tilde{v}_0 / \|\tilde{v}_0\|_a$ with \tilde{v}_0 the solution to the Poisson problem

$$\begin{cases} -\Delta \tilde{v}_0(\mathbf{x}) = \mathbf{1}_{\Omega_1}(\mathbf{x}) - \mathbf{1}_{\Omega_2}(\mathbf{x}), & \mathbf{x} \in \Omega, \\ \tilde{v}_0(\mathbf{x}) = 0, & \mathbf{x} \in \partial\Omega, \end{cases} \quad (6.3)$$

where $\mathbf{1}(\mathbf{x})$ is the indicator function and Ω_1, Ω_2 are two selected disjoint subdomains of Ω to control the convexity of v_0 . A numerical solution is reached at $w_k = p(v_k)$ by the NWP-LMM algorithm when $\|g_k\|_a = \|\nabla E(w_k)\|_a \leq 10^{-5}$ and $\max_{\mathbf{x} \in \Omega} |\Delta w_k(\mathbf{x}) - a(\mathbf{x})w_k(\mathbf{x}) + f(\mathbf{x}, w_k(\mathbf{x}))| \leq 5 \times 10^{-5}$. Particularly, it is necessary to explain more about how to numerically compute the gradient of the energy functional and a peak selection in numerical experiments. According to the definition of the gradient $g_k = \nabla E(w_k)$ of E at $w_k \in H$ in (5.1) and the definition of the inner product $(\cdot, \cdot)_a$ in (6.2), the gradient g_k can be expressed as $g_k = w_k - \phi_k$ with ϕ_k determined by the linear elliptic BVP

$$\begin{cases} -\Delta \phi_k(\mathbf{x}) + a(\mathbf{x})\phi_k(\mathbf{x}) = f(\mathbf{x}, w_k(\mathbf{x})), & \mathbf{x} \in \Omega, \\ \phi_k(\mathbf{x}) = 0, & \mathbf{x} \in \partial\Omega, \end{cases} \quad (6.4)$$

which can be solved efficiently by a standard numerical method, such as the finite element method (FEM) or the finite difference method. In our numerical code, **assempte**, a FEM-based subroutine provided by the MATLAB PDE Toolbox, is implemented to accomplish this task. The square domain in Cases 1-2 and the

dumbbell-shaped domain in Case 3 are, respectively, discretized with 32768 and 15552 triangular elements. In addition, the computation of a peak selection $p(v_k)$ of E at $v_k \in S_H$ w.r.t. a given $(n-1)$ -dimensional closed subspace L ($n \geq 1$) is an optimization problem in the n -dimensional half subspace $[L, v_k]$. To do this, a MATLAB subroutine `fminunc` with the termination tolerance on the first-order optimality $\text{To1} = 10^{-8}$ is called in our numerical code.

Further, for the convenience of numerical comparisons, we introduce the following notations for three different algorithms:

- **SD-Armijo**: the traditional LMM algorithm by utilizing the steepest descent direction $d_k = -g_k$ and the normalized Armijo-type step-size search rule [18, 32]. At each iterative step of this algorithm, the step-size α_k is chosen as

$$\alpha_k = \max_{m \in \mathbb{N}} \{ \lambda \rho^m : E(p(v_k(\lambda \rho^m))) \leq E(p(v_k)) - \sigma \lambda \rho^m t_k \|g_k\|^2 \}, \quad (6.5)$$

where constants σ, λ are fixed as $\sigma = 10^{-4}$ and $\lambda = 0.1$.

- **SD-StrongWolfe**: the NWP-LMM algorithm by utilizing the steepest descent direction $d_k = -g_k$ and the normalized strong Wolfe-Powell-type step-size search rule (3.12) with constants $\sigma_1 = 10^{-4}$ and $\sigma_2 = 0.4$.
- **CG-StrongWolfe**: the NWP-LMM algorithm by utilizing the CG-type direction (5.5) with $\beta_k = \beta_k^{\text{FR-like}}$ given in (5.8) and the normalized strong Wolfe-Powell-type step-size search rule (3.12) with constants $\sigma_1 = 10^{-4}$ and $\sigma_2 = 0.4$.

It is worthwhile to point out that it is generally not feasible to directly combine the CG-type direction and the Armijo-type step-size search rule in the LMM (i.e., d_k is not guaranteed to be a descent direction) as observed numerically.

6.1 Numerical results for the nonlinear Schrödinger equation

In this subsection, we report numerical results of Case 1, i.e., the NLSE in the focusing regime on the square domain $\Omega = (-1, 1)^2$ as

$$\begin{cases} -\Delta u(\mathbf{x}) + \omega |\mathbf{x}|^2 u(\mathbf{x}) = u^3(\mathbf{x}), & \mathbf{x} \in \Omega, \\ u(\mathbf{x}) = 0, & \mathbf{x} \in \partial\Omega. \end{cases} \quad (6.6)$$

Taking $\omega = 8$, limited by paper length, only ten different solutions labeled by u_1, u_2, \dots, u_{10} are shown in Fig. 4 for their profiles and features. The corresponding information on the support space L , subdomains Ω_1 and Ω_2 used in (6.3), and energy values of these solutions is listed in Table 1. In addition, numerical comparisons of the **SD-StrongWolfe**, **CG-StrongWolfe** and **SD-Armijo** in terms of CPU times for computing these solutions of the NLSE are presented in Fig. 5.

From Figs. 4-5, Table 1 and additional results not shown here, we observe that three LMM algorithms considered are effective for finding multiple solutions of the NLSE in the focusing regime and the **CG-StrongWolfe** shows the best performance among its LMM companions. In addition, u_1 (Fig. 4(a)) is the only positive solution with the lowest energy value, i.e., it is the ground state solution.

Table 1: The information to corresponding solutions of the NLSE in Fig. 4.

u_n	$E(u_n)$	L	Ω_1 ($\Omega_2 = \Omega \setminus \Omega_1$)	Graphics
u_1	14.7889	$\{0\}$	Ω	Fig. 4(a)
u_2	73.8223	$[u_1]$	$\{x_1 > 0\}$	Fig. 4(b)
u_3	73.8223	$[u_1]$	$\{x_2 > 0\}$	Fig. 4(c)
u_4	70.9151	$[u_1]$	$\{x_1 + x_2 > 0\}$	Fig. 4(d)
u_5	70.9151	$[u_1]$	$\{x_1 - x_2 > 0\}$	Fig. 4(e)
u_6	210.0238	$[u_1, u_2]$	$\{ x_1 > 0.2\}$	Fig. 4(f)
u_7	178.2474	$[u_1, u_4]$	$\{ x_1 + x_2 > 0.3\}$	Fig. 4(g)
u_8	213.6423	$[u_1, u_2, u_3]$	$\{x_1 x_2 > 0\}$	Fig. 4(h)
u_9	243.2646	$[u_1, u_4, u_5]$	$\{ x_1 > x_2 \}$	Fig. 4(i)
u_{10}	306.4755	$[u_1, u_2, u_3, u_8]$	$\{x_1^2 + x_2^2 > 0.25\}$	Fig. 4(j)

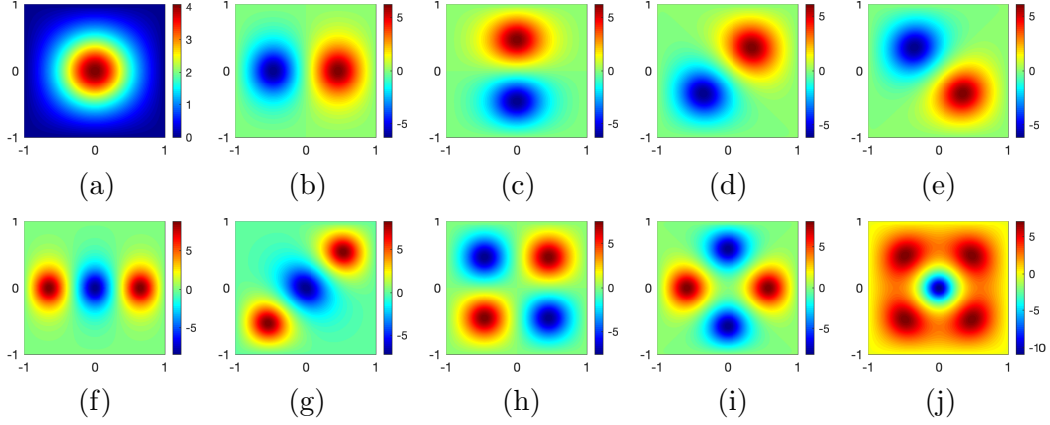


Figure 4: Profiles of ten different solutions of the NLSE: (a) the single-peak positive (ground state) solution u_1 concentrated mainly on the center of the domain; (b)–(j) nine multi-peak sign-changing solutions $u_2 \sim u_{10}$.

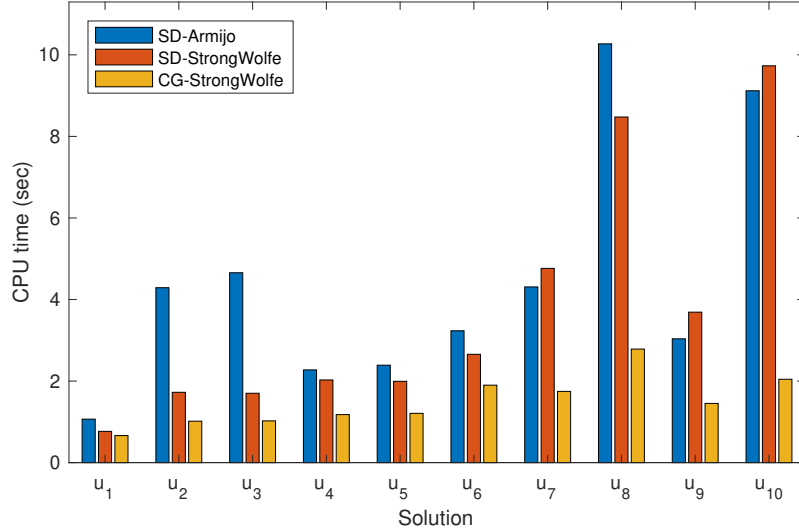


Figure 5: Comparison of CPU time of LMMs for finding solutions of the NLSE in Fig. 4.

Table 2: The information to corresponding solutions of the Hénon equation in Fig. 6.

u_n	$E(u_n)$	L	Ω_1	Ω_2	Graphics
u_1	61.9634	$\{0\}$	$\{x_1 > 0, x_2 > 0\}$	\emptyset	Fig. 6(a)
u_2	120.7887	$[u_1]$	$\{x_1 < 0, x_2 > 0\}$	\emptyset	Fig. 6(b)
u_3	122.4078	$[u_1]$	$\{x_1 < 0, x_2 < 0\}$	\emptyset	Fig. 6(c)
u_4	126.6988	$[u_1]$	$\{x_2 > 0\}$	\emptyset	Fig. 6(d)
u_5	125.3561	$[u_1]$	$\{x_1 > 0, x_2 > 0\}$	$\{x_1 < 0, x_2 < 0\}$	Fig. 6(e)
u_6	177.6068	$[u_1, u_2]$	$\{x_1 < 0, x_2 < 0\}$	\emptyset	Fig. 6(f)
u_7	187.1379	$[u_1, u_3]$	$\{x_2 > 0\}$	\emptyset	Fig. 6(g)
u_8	189.9406	$[u_1, u_4]$	$\{x_1 < 0, x_2 < 0\}$	\emptyset	Fig. 6(h)
u_9	230.0141	$[u_1, u_2, u_6]$	$\{x_1 > 0, x_2 < 0\}$	\emptyset	Fig. 6(i)
u_{10}	247.0220	$[u_1, u_2, u_6]$	$\{x_2 < 0\}$	$\{x_2 > 0\}$	Fig. 6(j)
u_{11}	250.6746	$[u_1, u_2, u_6]$	$\{x_1 x_2 > 0\}$	$\{x_1 x_2 < 0\}$	Fig. 6(k)
u_{12}	255.9728	$[u_1, u_2, u_6]$	$\{x_1 x_2 < 0\}$	\emptyset	Fig. 6(l)

6.2 Numerical results for the Hénon equation

Now, we report numerical results of Case 2, i.e., the Hénon equation on the square domain $\Omega = (-1, 1)^2$ as

$$\begin{cases} -\Delta u(\mathbf{x}) = |\mathbf{x}|^\ell u^3(\mathbf{x}), & \mathbf{x} \in \Omega, \\ u(\mathbf{x}) = 0, & \mathbf{x} \in \partial\Omega. \end{cases} \quad (6.7)$$

Fix $\ell = 6$, due to the space limitation, only twelve solutions we obtained, labeled by u_1, u_2, \dots, u_{12} , are displayed in Fig. 6 for their profiles and features. The corresponding information on the support space L , subdomains Ω_1 and Ω_2 used in (6.3), and energy values of these solutions is listed in Table 2. In addition, numerical comparisons of the **SD-StrongWolfe**, **CG-StrongWolfe** and **SD-Armijo** in terms of CPU times for computing these solutions of the Hénon equation are provided in Fig. 7.

From Figs. 6-7, Table 2 and additional results not shown here, we observe that three LMM algorithms considered can effectively find multiple solutions of the Hénon equation. As expected, the **CG-StrongWolfe** also shows the best performance among its LMM companions. In addition, positive solutions are not unique in the case of $\ell = 6$.

6.3 Numerical results for the Chandrasekhar equation

Here, we report numerical results of Case 3, i.e., the Chandrasekhar equation as

$$\begin{cases} -\Delta u(\mathbf{x}) = (u^2(\mathbf{x}) + 2u(\mathbf{x}))^{3/2}, & \mathbf{x} \in \Omega, \\ u(\mathbf{x}) = 0, & \mathbf{x} \in \partial\Omega. \end{cases} \quad (6.8)$$

We consider a dumbbell-shaped domain Ω as depicted in Fig. 8(a). It contains a smaller disk centered at $(-1, 0)$ with radius 0.5 and a larger disk centered at $(2, 0)$ with radius 1. A corridor of width 0.4, symmetric respect to the x_1 -axis, is constructed to link the two disks. In this case, we focus on finding multiple positive solutions. Limited by the length of the paper, we only present seven different positive solutions, labeled by u_1, u_2, \dots, u_7 , in Fig. 8(b)-(h) for their profiles and features. The corresponding information on the support space L , subdomains Ω_1 and Ω_2 used in (6.3), and energy values of these solutions is listed in Table 3. In addition, numerical comparisons of the **SD-StrongWolfe**, **CG-StrongWolfe** and **SD-Armijo** in terms of CPU times for computing these solutions of the Chandrasekhar equation

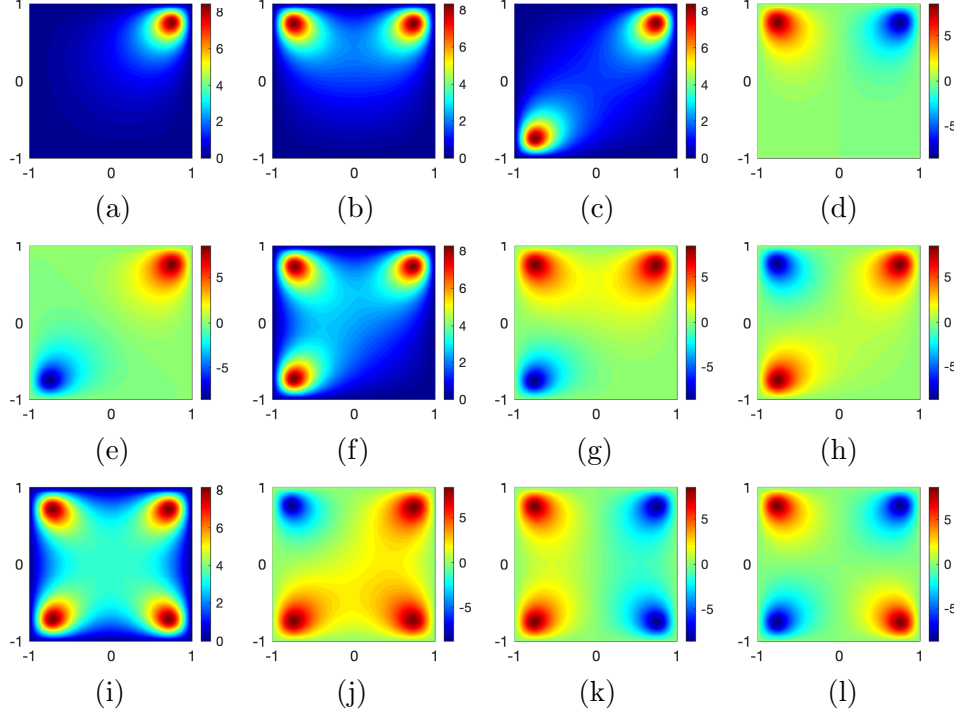


Figure 6: Profiles of twelve different solutions of the Hénon equation: (a) the single-peak positive (ground state) solution u_1 concentrated mainly on the corner; (b) a two-peak positive solution u_2 concentrated mainly on two adjacent corners; (c) a two-peak positive solution u_3 concentrated mainly on two diagonal corners; (d) a two-peak sign-changing solution u_4 concentrated mainly on two adjacent corners; (e) a two-peak sign-changing solution u_5 concentrated mainly on two diagonal corners; (f) a three-peak positive solution u_6 ; (g)-(h) two three-peak sign-changing solutions u_7 and u_8 ; (i) a four-peak positive solution u_9 ; (j)-(l) three four-peak sign-changing solutions u_{10} , u_{11} and u_{12} .

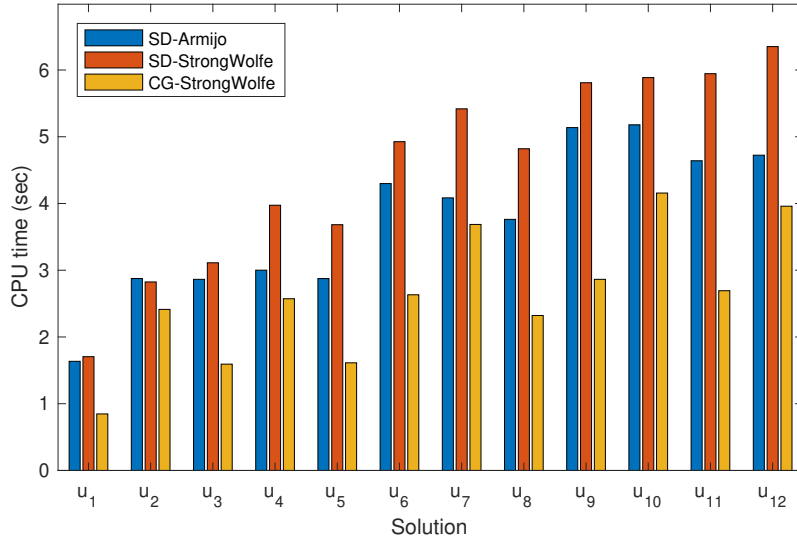


Figure 7: Comparison of CPU time of LMMs for finding solutions of the Hénon equation in Fig. 6.

Table 3: The information to corresponding solutions of the Chandrasekhar equation in Fig. 8.

u_n	$E(u_n)$	L	Ω_1 ($\Omega_2 = \emptyset$)	Graphics
u_1	1.6624	$\{0\}$	$\{(x_1 - 2)^2 + x_2^2 < 1\}$	Fig. 8(b)
u_2	18.0067	$\{0\}$	$\{(x_1 + 1)^2 + x_2^2 < 0.5\}$	Fig. 8(c)
u_3	108.0580	$\{0\}$	$\{(x_1 - 0.25)^2 + x_2^2 < 0.1\}$	Fig. 8(d)
u_4	19.6691	$[u_1]$	$\{(x_1 + 1)^2 + x_2^2 < 0.5\}$	Fig. 8(e)
u_5	109.6897	$[u_1]$	$\{(x_1 - 0.25)^2 + x_2^2 < 0.1\}$	Fig. 8(f)
u_6	125.8846	$[u_2]$	$\{(x_1 - 0.25)^2 + x_2^2 < 0.1\}$	Fig. 8(g)
u_7	127.5247	$[u_1, u_2]$	$\{(x_1 - 0.25)^2 + x_2^2 < 0.1\}$	Fig. 8(h)

Table 4: Comparison of the number of iterations (#its) and CPU time (time) in seconds of LMMs with different number of triangular elements (n_T) used in the FEM for computing the gradient direction g_k in the iterations for finding the solution u_1 of the Chandrasekhar equation in Fig. 8.

LMMs	SD-Armijo		SD-StrongWolfe		CG-StrongWolfe	
n_T	#its	time	#its	time	#its	time
3744	51	0.4329	13	0.1270	10	0.0978
6050	51	0.5782	13	0.1704	9	0.1314
9732	51	0.8287	13	0.2540	9	0.1757
15552	51	1.2944	13	0.3921	9	0.2843
55472	51	4.2249	13	1.2340	9	0.9055
152696	51	12.018	13	3.3641	9	2.4026
635658	51	72.296	13	19.660	9	14.258

are provided in Fig. 9. Finally, the comparison of the computational efficiency of the three LMMs by increasing the elements and then freedoms in the FEM for computing the gradient direction g_k in the iterations for finding u_1 are listed in Table 4.

From Figs. 8-9, Tables 3-4 and additional results not shown here, we observe that three LMM algorithms considered can effectively find multiple positive solutions of the Chandrasekhar equation. It is also observed that the FEM mesh size has little effect on the number of iterations of the three algorithms. Again, the CG-StrongWolfe also shows the best performance in this case.

Above all, numerical experiments in this section indicate that the CG-type direction indeed speed up the LMM greatly.

7 Conclusions

In this paper, we introduced a framework of normalized Wolfe-Powell-type local min-max method (NWP-LMM) based on general descent directions and the normalized Wolfe-Powell-type and strong Wolfe-Powell-type step-size search rules for finding multiple unstable solutions of semilinear elliptic problems. Under certain conditions on the local peak selection and general descent directions, the feasibility and global convergence of the NWP-LMM were rigorously verified in the functional analysis level. In addition, two feasible types of descent directions, i.e., preconditioned steepest descent directions and the conjugate gradient-type direction, were proposed and discussed. The global convergence of the NWP-LMM combined with the preconditioned steepest descent directions was also provided. Extensive numerical results for several semilinear elliptic equations, including the nonlinear Schrödinger equation, Hénon equation and Chandrasekhar equation in 2D, were reported with their

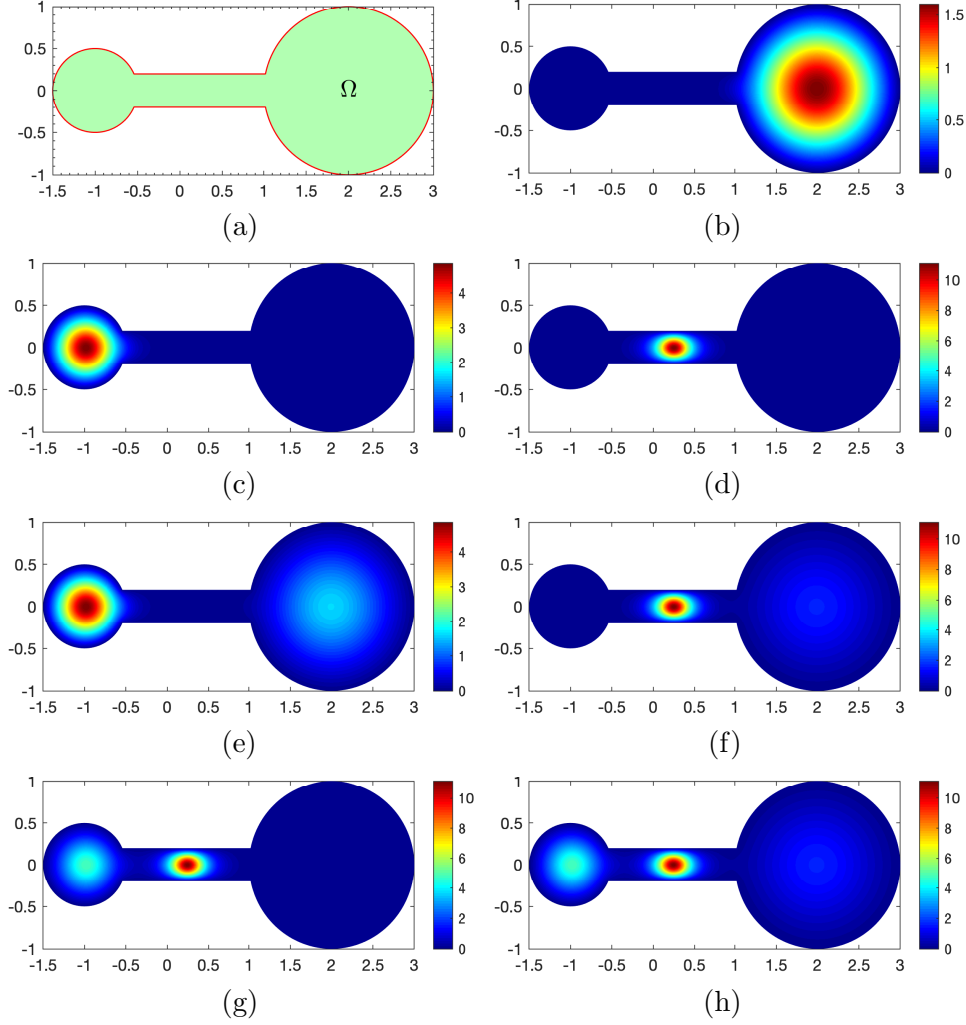


Figure 8: (a) A dumbbell-shaped domain. (b)-(h) Profiles of seven different positive solutions of the Chandrasekhar equation: (b) the single-peak positive ground state solution u_1 concentrated mainly on the larger disk; (c) a single-peak positive solution u_2 concentrated mainly on the smaller disk; (d) a single-peak positive solution u_3 concentrated mainly on the corridor; (e)-(g) three two-peak positive solutions u_4 , u_5 and u_6 ; (h) a three-peak positive solution u_7 .

multiple solutions displayed to illustrate the effectiveness and robustness of our approach. The superior numerical performance of the NWP-LMM combined with the conjugate gradient-type direction was observed in extensive numerical experiments, while the rigorous verification for its global convergence is ongoing. Furthermore, designing more efficient preconditioned steepest descent or preconditioned conjugate gradient-type directions within the framework of LMM by constructing appropriate preconditioners to further improve the efficiency of computing multiple solutions will be our future work. Finally, it is worthwhile to point out that, following the line of our approach, the steepest descent direction can be replaced by a general descent direction in the devise of the traditional normalized Armijo-type and Goldstein-type local minimax algorithms, and both the feasibility and global convergence of the them can be verified.

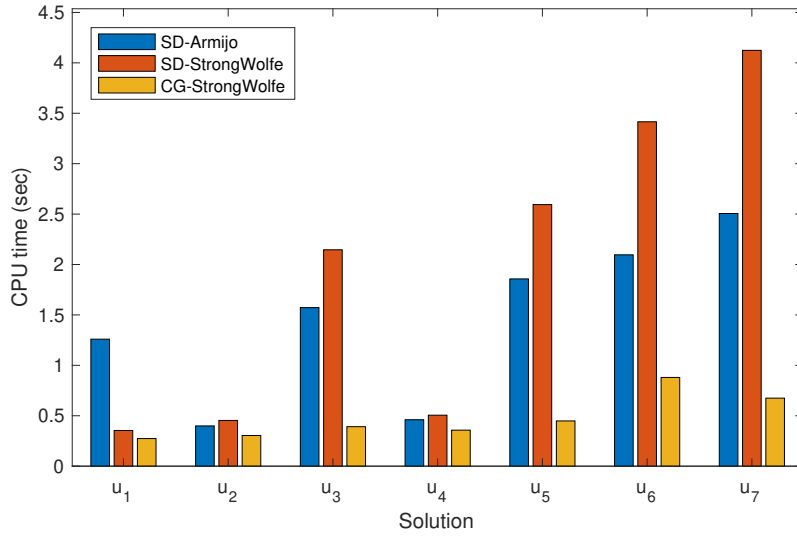


Figure 9: Comparison of CPU time of LMMs for finding solutions of the Chandrasekhar equation in Fig. 8.

References

- [1] M. Al-Baali. Descent property and global convergence of the Fletcher-Reeves method with inexact line search. *IMA J. Numer. Anal.*, 5(1):121–124, 1985.
- [2] K.-C. Chang. *Infinite Dimensional Morse Theory and Multiple Solution Problems*. Birkhäuser Boston, 1993.
- [3] C. Chen and Z. Xie. Search extension method for multiple solutions of a nonlinear problem. *Comput. Math. Appl.*, 47:327–343, 2004.
- [4] C. Chen and Z. Xie. Analysis of search-extension method for finding multiple solutions of nonlinear problem. *Sci. China Ser. A-Math.*, 51(1):42–54, 2008.
- [5] G. Chen, J. Zhou, and W.-M. Ni. Algorithms and visualization for solutions of nonlinear elliptic equations. *Internat. J. Bifur. Chaos*, 10(07):1565–1612, 2000.
- [6] Y. S. Choi and P. J. McKenna. A mountain pass method for the numerical solution of semilinear elliptic problems. *Nonlinear Anal. Theor. Meth. Appl.*, 20(4):417–437, 1993.
- [7] Y. Dai and Y.-X. Yuan. *Nonlinear Conjugate Gradient Methods (in Chinese)*. Shanghai Scientific & Technical Publishers, 2000.
- [8] F. Dalfovo, S. Giorgini, L. P. Pitaevskii, and S. Stringari. Theory of Bose-Einstein condensation in trapped gases. *Rev. Mod. Phys.*, 71:463–512, 1999.
- [9] Z. Ding, D. Costa, and G. Chen. A high-linking algorithm for sign-changing solutions of semilinear elliptic equations. *Nonlinear Anal.*, 38(2):151–172, 1999.
- [10] W. E, W. Ren, and E. Vanden-Eijnden. String method for the study of rare events. *Phys. Rev. B*, 66(5):052301, 2002.
- [11] W. E and X. Zhou. The gentlest ascent dynamics. *Nonlinearity*, 24(6):1831–1842, 2011.
- [12] R. Fletcher. *Practical Methods of Optimization*. John Wiley & Sons, Chichester, 1987.
- [13] R. Fletcher and C. M. Reeves. Function minimization by conjugate gradients. *Comput. J.*, 7(2):149–154, 1964.
- [14] W. Hager and H. Zhang. A survey of nonlinear conjugate gradient methods. *Pac. J. Optim.*, 2(1):35–58, 2006.
- [15] G. Henkelman and H. Jónsson. A dimer method for finding saddle points on high dimensional potential surfaces using only first derivatives. *J. Chem. Phys.*, 111(15):7010–7022, 1999.
- [16] A. Le, Z.-Q. Wang, and J. Zhou. Finding multiple solutions to elliptic PDE with nonlinear boundary conditions. *J. Sci. Comput.*, 56(3):591–615, 2013.
- [17] Y. Li and J. Zhou. A minimax method for finding multiple critical points and its applications to semilinear PDEs. *SIAM J. Sci. Comput.*, 23(3):840–865, 2001.

- [18] Y. Li and J. Zhou. Convergence results of a local minimax method for finding multiple critical points. *SIAM J. Sci. Comput.*, 24(3):865–885, 2002.
- [19] Z. Li, Z.-Q. Wang, and J. Zhou. A new augmented singular transform and its partial Newton-correction method for finding more solutions. *J. Sci. Comput.*, 71(2):634–659, 2017.
- [20] W. Liu, Z. Xie, and W. Yi. Normalized Goldstein-type local minimax method for finding multiple unstable solutions of semilinear elliptic PDEs. *Commun. Math. Sci.*, 19(1):147–174, 2021.
- [21] W. Liu, Z. Xie, and Y. Yuan. Convergence analysis of a spectral-Galerkin-type search extension method for finding multiple solutions of semilinear problems (in Chinese). *Sci. Sin. Math.*, 51(9):1407–1431, 2021.
- [22] W. Liu, Z. Xie, and Y. Yuan. A constrained gentlest ascent dynamics and its applications to finding excited states of Bose–Einstein condensates. *J. Comput. Phys.*, 473:111719, 2023.
- [23] J. Nocedal and S. J. Wright. *Numerical Optimization, Springer Series in Operations Research and Financial Engineering*. Springer, New York, 2nd edition, 2006.
- [24] M. J. D. Powell. Some global convergence properties of a variable metric algorithm for minimization without exact line searches. In *Nonlinear Programming* (R. W. Cottle and C. E. Lemke eds.). SIAM-AMS Proc., Vol. IX. SIAM Publications, Philadelphia, 53–72, 1976.
- [25] P. H. Rabinowitz. *Minimax Methods in Critical Point Theory with Applications to Differential Equations*. CBMS Reg. Conf. Ser. Math., No. 65, Amer. Math. Soc., Providence, R. I., 1986.
- [26] W. Ren and E. Vanden-Eijnden. A climbing string method for saddle point search. *J. Chem. Phys.*, 138(13):134105, 2013.
- [27] W. Sun and Y.-X. Yuan. *Optimization Theory and Methods: Nonlinear Programming*. Springer, 2006.
- [28] P. Wolfe. Convergence conditions for ascent methods. *SIAM Rev.*, 11(2):226–235, 1969.
- [29] P. Wolfe. Convergence conditions for ascent methods. II: Some corrections. *SIAM Rev.*, 13(2):185–188, 1971.
- [30] Z. Xie, C. Chen, and Y. Xu. An improved search-extension method for computing multiple solutions of semilinear PDEs. *IMA J. Numer. Anal.*, 25(3):549–576, 2005.
- [31] Z. Xie, W. Yi, and J. Zhou. An augmented singular transform and its partial Newton method for finding new solutions. *J. Comput. Appl. Math.*, 286:145–157, 2015.
- [32] Z. Xie, Y. Yuan, and J. Zhou. On finding multiple solutions to a singularly perturbed Neumann problem. *SIAM J. Sci. Comput.*, 34(1):A395–A420, 2012.
- [33] X. Yao and J. Zhou. A minimax method for finding multiple critical points in Banach spaces and its application to quasi-linear elliptic PDE. *SIAM J. Sci. Comput.*, 26(5):1796–1809, 2005.
- [34] J. Yin, Z. Huang, and L. Zhang. Constrained high-index saddle dynamics for the solution landscape with equality constraints. *J. Sci. Comput.*, 91:62, 2022.
- [35] J. Yin, B. Yu, and L. Zhang. Searching the solution landscape by generalized high-index saddle dynamics. *Sci. China Math.*, 64:1801–1816, 2021.
- [36] J. Yin, L. Zhang, and P. Zhang. High-index optimization-based shrinking dimer method for finding high-index saddle points. *SIAM J. Sci. Comput.*, 41(6):A3576–A3595, 2019.
- [37] J. Zhang and Q. Du. Shrinking dimer dynamics and its applications to saddle point search. *SIAM J. Numer. Anal.*, 50(4):1899–1921, 2012.
- [38] L. Zhang, W. Ren, A. Samanta, and Q. Du. Recent developments in computational modelling of nucleation in phase transformations. *npj Comput. Mater.*, 2:16003, 2016.
- [39] J. Zhou. Solving multiple solution problems: computational methods and theory revisited. *Commun. Appl. Math. Comput.*, 31(1):1–31, 2017.